

# Low-pressure radio-frequency inductive discharge and possibilities of optimizing inductive plasma sources

E A Kral'kina

DOI: 10.1070/PU2008v051n05ABEH006422

## Contents

<b>1. Introduction</b>	<b>493</b>
<b>2. Power absorption by radio-frequency inductive discharge plasmas</b>	<b>495</b>
<b>3. Equivalent plasma resistance</b>	<b>496</b>
3.1 Definition and methods of calculation; 3.2 Measuring techniques; 3.3 Inductive discharge without an external magnetic field; 3.4 Inductive discharge with an external magnetic field	
<b>4. Properties of a low-pressure radio-frequency inductive discharge operating in the <math>R_{pl} \leq R_{ant}</math> regime</b>	<b>500</b>
4.1 Dependence of plasma parameters on the radio-frequency plasma source power; 4.2 Dependence of plasma parameters on the external magnetic field	
<b>5. Properties of a radio-frequency inductive discharge with a capacitive component</b>	<b>506</b>
5.1 Dependence of plasma parameters on the radio-frequency plasma source power; 5.2 Dependence of plasma parameters on the external magnetic field; 5.3 Hybrid discharge	
<b>6. On the feasibility of optimizing low-pressure inductive plasma sources</b>	<b>510</b>
<b>7. Conclusion</b>	<b>511</b>
<b>References</b>	<b>512</b>

**Abstract.** Plasma reactors and ion sources whose operation relies on a low-pressure radio-frequency (RF) inductive discharge have been an important constituent of modern ground and space technologies for several decades already. However, the steadily toughening and varying requirements of plasma technologies call for improving the old models of devices and developing novel prospective models. Of vital importance in the development of inductive plasma sources is the provision of conditions whereat the plasma efficiently absorbs the RF power. In recent years it has become evident that in a low-pressure RF inductive discharge the RF-generator power is distributed between the active resistance of the external circuit and the plasma. In the latter case, the power is delivered to the plasma via two channels: an inductive channel, which exists due to the current flowing through an inductor or an antenna, and a capacitive one, which is due to the antenna–plasma capacitive coupling. RF inductive discharge properties related to the RF-power redistribution between the channels are considered and the mechanisms of RF-power absorption are analyzed. The feasibilities of optimizing RF inductive plasma sources are also discussed.

## 1. Introduction

Among the most important problems in the organization of plasma technological processes is the development of plasma sources possessing optimal properties for a given technology, for instance, a high uniformity, prescribed plasma density, charged particle energy, and the concentration of chemically active radicals. An analysis suggests that radio-frequency (RF) plasma sources show the greatest promise for industrial technologies, because, first, both conductive and dielectric materials can be processed with their aid and, second, not only inert gases can be employed as the working gas, but chemically active gases as well. Presently known are plasma sources which rely on capacitive and inductive RF discharges. The capacitive RF-discharge peculiarity most frequently employed in plasma technologies is the existence of near-electrode space-charge layers in which there forms the time-average drop in electric potential that accelerates ions towards the electrode. This permits processing the material specimens located at the electrodes of a capacitive RF discharge by means of accelerated ions. Another peculiarity of the capacitive discharge quite frequently employed in applications is the production of a large number of fast electrons in the near-electrode layers of the space charge. The presence of fast electrons in the discharge is responsible for the efficient dissociation of complex molecules and the production of radicals which are required for the reactive etching of materials, plasma-induced polymerization, etc. A disadvantage of the capacitive RF discharge is the relatively low electron concentration in the main plasma volume. Inductive RF discharges are characterized by a significantly higher electron concentration for the same RF power.

E A Kral'kina M V Lomonosov Moscow State University,  
Department of Physics,  
Vorob'evy gory, 119992 Moscow, Russian Federation  
Tel. (7-495) 939 47 73  
E-mail: ekralkina@mail.ru

Received 25 June 2007, revised 12 November 2007  
*Uspekhi Fizicheskikh Nauk* 178 (5) 519–540 (2008)  
DOI: 10.3367/UFNr.0178.200805f.0519  
Translated by E N Ragozin; edited by A Radzig

Inductive RF discharge without a magnetic field has been known for more than a century [1, 2]. This is a discharge initiated by the current flowing through the inductor located on the side or end surface of, as a rule, a cylindrical plasma source. Away back in 1891, J J Thomson hypothesized [1] that the inductive discharge was caused and maintained by the vortex electric field produced by the RF magnetic field which, in turn, is induced by the current flowing through the antenna. In 1928–1929, J J Thomson's view was challenged by J Townsend and R Donaldson [3, 4], who came up with the idea that the inductive RF discharge was maintained not by vortex electric fields, but by potential fields which emerge due to the potential difference between the inductor turns. In 1929, K MacKinnon [5] showed experimentally the existence of the two discharge regimes. For low amplitudes of the RF voltage, the discharge did occur under the action of an electric field between the coil turns and exhibited a weak longitudinal glow along the length of the gas-discharge tube. With an increase in the RF voltage amplitude, the glow became brighter and finally a bright circular discharge emerged. The glow caused by the longitudinal electric field disappeared in this case. These two forms of the discharge were later termed the *E* and *H* discharges, respectively.

The domain of existence of the inductive discharge may be conventionally divided into two large ones [6]: with high pressures (on the order of atmospheric pressure) where at the generated plasma is nearly equilibrium, and with low pressures at which the generated plasma is nonequilibrium. The subject of this paper covers the second domain of existence of the RF inductive discharge.

Plasma reactors and ion sources which operate using a low-pressure RF inductive discharge have been an important constituent of modern ground and space technologies for several decades. The widespread use of the technical applications of the RF inductive discharge is fostered by its main virtues, namely, the possibility of obtaining a high electron concentration for a relatively low level of RF power, the absence of contact between the plasma and metallic electrodes, and a low electron temperature and hence a moderate plasma potential relative to the discharge-confining walls. The last one permits, apart from minimizing the power loss at the walls of the plasma source, obviating the surface damage of the specimens in their processing by high-energy ions in the discharge.

Presently known are low-pressure plasma sources whose operation relies on an RF inductive discharge in the absence of a magnetic field, as well as on an RF inductive discharge embedded in an external magnetic field, with induction corresponding to the conditions of electron cyclotron resonance (ECR) and the excitation conditions for helicons and Trivelpiece–Gold (TG) waves (hereinafter referred to as helicon sources).

Typical examples of plasma sources involving an RF inductive discharge without a magnetic field are plasma reactors intended for substrate etching [7], ion sources intended for the realization of earthly ion-beam technologies and for work in space as orbit correction engines for space vehicles [8], and light sources [9]. The common design feature of the above devices is the existence of a gas-discharge chamber (GDC) with an inductor or an antenna located on its outer surface or inside of it. The antenna is connected to the radio-frequency plasma source and serves to deposit the RF power into the GDC volume and ignite

the electrodeless discharge. The currents flowing through the antenna induce in the plasma a vortex electric field which heats electrons to energies required to efficiently ionize the working gas. Typical plasma densities range from  $10^{11}$  to  $3 \times 10^{12} \text{ cm}^{-3}$  in the plasma reactors, and from  $3 \times 10^{10}$  to  $3 \times 10^{11} \text{ cm}^{-3}$  in the ion sources. The typical neutral gas pressure varies between 1 and 30 mTorr in plasma reactors; it is close to 0.1 mTorr in ion sources, and ranges 0.1–10 Torr in light sources.

It is well known that the RF electric fields in an inductive discharge plasma are confined to the skin layer, i.e., the electrons are heated in a narrow near-wall layer. When an external magnetic field is applied to the RF inductive discharge plasma there appear transparency domains in which the RF fields penetrate to the plasma interior and the electrons are heated in the entire plasma volume. This effect is employed in plasma sources whose operation relies on ECR. These sources operate primarily in the microwave (2.45 GHz) range [10]. The microwave radiation is fed, as a rule, through a quartz window to a cylindrical gas-discharge chamber in which magnets form a nonuniform magnetic field. The magnetic field is characterized by the existence of one or several resonance zones in which the ECR conditions are fulfilled, and the RF power is delivered to the plasma. In the radio-frequency range, ECR is employed in the so-called plasma sources with a neutral loop [11–16]. The neutral loop, which comprises a continuous sequence of points with a zero magnetic field, plays an important part in plasma generation and the formation of discharge structure. The closed magnetic circuit is formed with the aid of three electromagnets. The currents in the windings of the upper and lower coils flow in the same direction. The current in the medium coil flows in the opposite direction. The RF inductive discharge with a neutral circuit is characterized by a high plasma density ( $10^{11}$ – $10^{12} \text{ cm}^{-3}$ ) and a low electron temperature (1–4 eV).

Another type of sources that employ an RF inductive discharge with an external magnetic field is helicon plasma sources [17, 18] which ordinarily consist of two hollow cylinders made of a dielectric material. Mounted on the outer lateral area of the smaller-diameter cylinder is the antenna, whose shape is optimal for the excitation of helicons and TG waves. The waves enter the larger-diameter chamber along the axial magnetic field produced by the magnetic system. The typical plasma concentration in helicon sources amounts to  $10^{12} \text{ cm}^{-3}$ , the magnetic field induction is on the order of 500–1000 G, and the RF power comes to 2–3 kW.

Aleksandrov et al. [19, 20] reported a plasma reactor and an ion source operating under the conditions where the helicon is a surface wave and the TG wave penetrates to the plasma interior. The ion source [20] affords an ion current density of 0.5 to 3 mA  $\text{cm}^{-2}$  for an RF power level not exceeding 150 W. The magnetic field intensity is equal to 200–300 G.

We summarize the above plasma parameters typical for inductive plasma sources. As a rule, the radius  $r$  of RF plasma sources ranges from 2 to 25 cm, and the length  $L$  from 3 to 50 cm. The plasma density  $n_e$  varies within the range from  $1 \times 10^{10}$  to  $3 \times 10^{12} \text{ cm}^{-3}$  for an electron temperature  $T_e \sim 3$ –8 eV ( $3 \times 10^4$ – $9 \times 10^4$  K). The neutral gas pressure  $p$  in the sources (with the exception of light sources) ranges from 0.1 to 10 mTorr. The magnetic field induction varies from zero up to 1 kG. In this paper, the properties of RF inductive

discharges are analyzed within these ranges of plasma parameters.

Estimates suggest that the electron collision frequency  $\nu$  under the above conditions, i.e., for relatively low plasma densities, is defined by the electron–atom collision frequency  $\nu_{ea}$ , the electron–ion collision frequency  $\nu_{ei}$  becoming significant only at a density  $n_e$  exceeding  $10^{12} \text{ cm}^{-3}$ . The quantity  $k\nu_{Te}$ , which characterizes the Cherenkov absorption ( $k$  is the wave vector, and  $\nu_{Te}$  is the electron thermal velocity), is close in magnitude to the electron–atom collision frequency. Therefore, both the collisional and Cherenkov mechanisms make contributions to absorption in a low-pressure RF inductive discharge.

Despite the large number of the schemes of plasma devices operating by the RF inductive discharge, the steadily toughening and varying requirements on plasma technologies call for improving the old models of devices and developing novel prospective models. This task poses a number of questions for the developers of plasma sources.

- What discharge scheme — a discharge without a magnetic field or a discharge embedded in the magnetic field corresponding to ECR, the helicon and TG wave excitation conditions — should be adopted when developing a plasma source for a specific technological application?
- How can the RF power absorption by the plasma be optimized and efficient power input be ensured?
- How is it possible to afford the reproducibility and reliability of plasma source operation?
- How can the highest possible plasma density in the source be obtained for given levels of the power absorbed by the plasma and the working gas flow rate?
- What external factors permit obtaining the preselected plasma density distribution and/or the spatial current density distribution in the ion beam?

It is evident that the answers to the above-formulated questions may be provided only on the basis of the fundamental knowledge of the physical processes occurring in the RF inductive discharge [21–38]. Let us consider the main notions of the physical processes that proceed in the low-pressure RF inductive discharge and then in Section 6 we will endeavor to provide the answers to the questions posed above.

## 2. Power absorption by radio-frequency inductive discharge plasmas

An RF inductive discharge constitutes the discharge excited by the current flowing through an inductor located on the lateral or end surface of, as a rule, a cylindrical plasma source (Figs 1a, b). The central question of the physics of the low-pressure inductive discharge is that of the mechanisms and efficiency of RF-power absorption by the plasma. Even since the time of J J Thomson it has been known [39] that the equivalent circuit of the RF discharge under purely inductive excitation may be represented in the form depicted in Fig. 1d. An RF plasma source is loaded on a transformer whose primary winding consists of an antenna carrying the current produced by the generator, and its secondary winding is the current induced in the plasma. The primary and secondary transformer windings are coupled by the mutual inductance coefficient  $M$ . The transformer circuit may be easily reduced to a scheme which is made up of the active resistance and inductance of the antenna, the equivalent plasma resistance and inductance connected in series (Fig. 1e), so that the RF

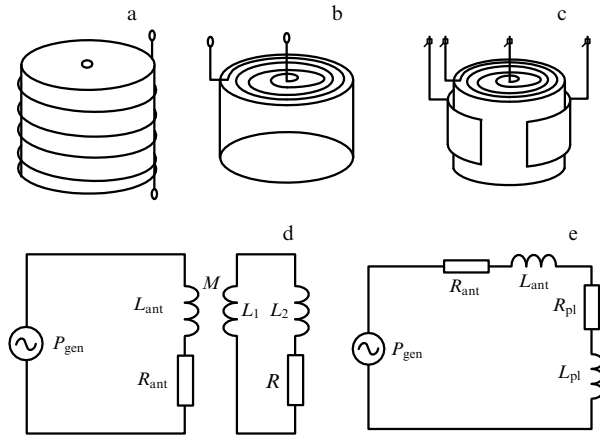


**Figure 1.** Schemes (a, b) of inductive plasma sources, and (c) of an inductive plasma source with a capacitive component; (d, e) equivalent circuits of a purely inductive discharge.

generator (plasma source) power  $P_{gen}$ , the power  $P_{ant}$  released in the antenna, and the power  $P_{pl}$  released in the plasma turn out to be related by the expressions

$$P_{gen} = P_{ant} + P_{pl}, \tag{1}$$

$$P_{gen} = \frac{1}{2} I^2 (R_{ant} + R_{pl}), \tag{2}$$

where  $I$  is the current flowing through the antenna,  $R_{ant}$  is the active antenna resistance, and  $R_{pl}$  is the equivalent plasma resistance.

As is clear from formulas (1) and (2), when the load is matched to the generator the active RF power  $P_{gen}$  which the generator imparts to the external circuit is distributed between two channels: specifically, one part of the power goes into antenna heating, and the other part is absorbed by the plasma. In the majority of earlier papers it was *a priori* assumed that under experimental conditions

$$R_{pl} \gg R_{ant}, \tag{3}$$

and the plasma properties were determined by the RF-generator power which was completely absorbed by the plasma. In the mid-1990s, V Godyak and his coworkers showed conclusively [40] that relation (3) may be violated in low-pressure discharges. It is evident that under the condition

$$R_{pl} \leq R_{ant} \tag{4}$$

the behavior of the RF inductive discharge will be radically different. In this case, the plasma parameters depend not only on the RF-generator power, but also on the equivalent plasma resistance which, in turn, depends on the plasma parameters and the conditions of plasma maintenance. This gives rise to the appearance of new effects related to the self-consistent power redistribution in the external discharge circuit. The latter may strongly affect the operation efficiency of plasma sources. Clearly, the key to the understanding of discharge behavior in the regimes corresponding to inequality (4), as well as to the optimization of plasma device operation, lies with the laws of the variation in equivalent plasma resistance under the variation in plasma parameters and the conditions of discharge maintenance.

### 3. Equivalent plasma resistance

#### 3.1 Definition and methods of calculation

In the general case, the RF power absorbed by the plasma is defined by the expression [22]

$$P_{\text{pl}} = \frac{L\omega}{4} \int_0^R r [\varepsilon_{\perp}'' |E_r|^2 + \varepsilon_{\perp}'' |E_{\phi}|^2 + \varepsilon_{\parallel}'' |E_z|^2 + g'' (E_{\phi} E_r^* - E_r E_{\phi}^*)] dr, \quad (5)$$

where  $E_{\phi}$ ,  $E_r$ , and  $E_z$  are the azimuthal, radial, and longitudinal components of the RF electric field strength in the plasma, respectively, and  $\varepsilon_{\perp}''$ ,  $\varepsilon_{\parallel}''$ , and  $g''$  are the imaginary parts of the components of the plasma permittivity tensor. The integration is performed over the entire plasma volume. In an inductive discharge, the RF electric fields are proportional to the current carried by the antenna, and therefore expression (5) may be rewritten in the form

$$P_{\text{pl}} = \frac{1}{2} R_{\text{pl}} I^2, \quad (6)$$

where the proportionality coefficient  $R_{\text{pl}}$  has the dimensionality of resistance and depends only on the plasma parameters.

A comparison of expression (6) with formula (2), which was obtained proceeding from the transformer discharge model, shows that the proportionality coefficient in expression (6) represents the equivalent plasma resistance.

From formulas (5) and (6) it is clear that the physical meaning of the equivalent plasma resistance lies in the fact that this resistance is the measure of the ability of plasma to absorb RF power. The magnitude of equivalent resistance depends both on the laws of field penetration into the plasma and on the mechanism of power absorption, i.e., it is dictated by the main fundamental properties of inductive discharge plasma.

From formula (5) it is evident that the RF fields in the plasma volume should be known if we are to calculate the equivalent resistance. These fields may be found proceeding from the theoretical models of low-pressure inductive plasma sources [41–45].

#### 3.2 Measuring techniques

When the discharge is purely inductive and the load is matched to the generator, the RF power  $P_{\text{gen}}$  imparted by the generator to the external circuit is distributed between two channels, namely, a part of the power goes into heating the antenna and the other part is absorbed by the plasma [25, 40]. In reality, the antenna resistance in experiments comprises the losses due to the heating of the elements of the matching system, the antenna itself, metallic facility parts located in the vicinity of the plasma source through the excitation of inductive currents in them, RF connectors, etc. That is why the technique of measuring  $R_{\text{pl}}$  involves the following stages. At first, the effective antenna resistance is determined from the measured values of the RF-generator power and the current  $I_0$  carried by the antenna without a discharge:

$$R_{\text{ant}} = \frac{2P_{\text{gen}}}{I_0^2}. \quad (7)$$

Then, the total resistance  $R$  of the external circuit is calculated from the antenna current and the RF-generator power measured during the discharge:

$$R = \frac{2P_{\text{gen}}}{I^2}. \quad (8)$$

The antenna resistance is subtracted from the total resistance of the external circuit to give the equivalent plasma resistance

$$R_{\text{pl}} = \frac{2P_{\text{gen}}}{I^2} - R_{\text{ant}}. \quad (9)$$

The fraction of RF power absorbed by the plasma is easily calculated from the known equivalent plasma resistance:

$$P_{\text{pl}} = \frac{1}{2} R_{\text{pl}} I^2. \quad (10)$$

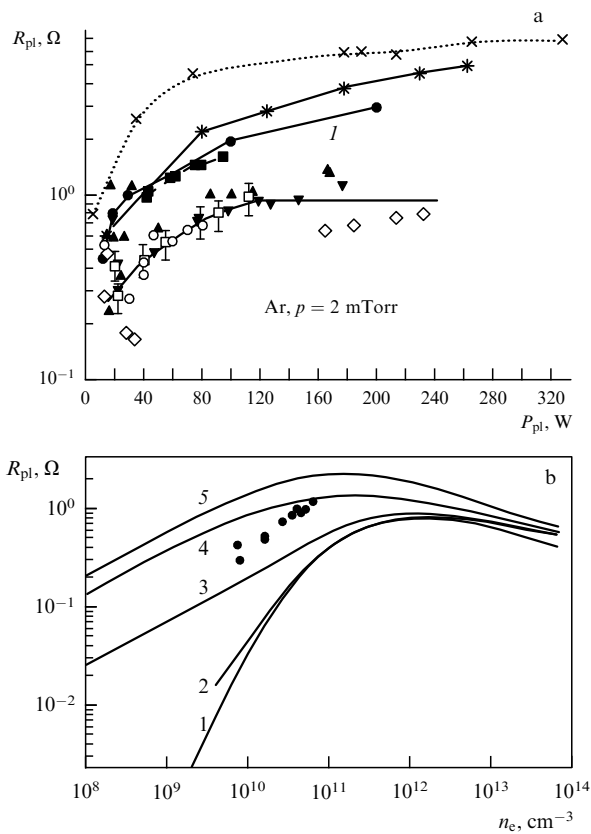
#### 3.3 Inductive discharge without an external magnetic field

Figure 2a shows the values of equivalent plasma resistance of an RF inductive discharge [46, 47] obtained in experiments with the plasma sources of various sizes at an argon pressure close to 2 mTorr. The power  $P_{\text{pl}}$  absorbed by the plasma is plotted on the abscissa as an independent variable. It would appear reasonable that the plasma density  $n_e$  would be proportional to  $P_{\text{pl}}$ ; however, it is pertinent to note that the coefficients of proportionality between  $P_{\text{pl}}$  and  $n_e$  would be different for various plasma sources. One can see that the common behavioral tendency of the equivalent resistance  $R_{\text{pl}}$  is its increase in the range of relatively low values of energy deposition, with its subsequent saturation.

Figure 2b depicts the equivalent plasma resistance as a function of electron concentration calculated in the framework of the kinetic model of a low-density RF inductive plasma source without a magnetic field [42, 45]. The calculated values of equivalent resistance are somewhat lower than the measured ones [46]. Despite the quantitative discrepancy, the experimental and calculated  $R_{\text{pl}}(n_e)$  dependences are qualitatively close to each other. In the domain of low plasma densities  $n_e$ , the calculated  $R_{\text{pl}}$  values, like the experimental ones, rise proportionally with  $n_e$  and then become saturated. In the region of high electron concentrations, which were not attained experimentally, the calculated  $R_{\text{pl}}$  pass through a maximum and then show a slow decrease.

At low pressures, the region of low electron concentrations corresponds to the case of weak spatial dispersion, and therefore the dependence  $R_{\text{pl}}(n_e)$  is adequately approximated by the data calculated using expressions for the permittivity obtained for a medium without spatial dispersion [42, 45]. By contrast, in the region of high electron concentrations, where collisionless absorption prevails, i.e., in the domain of the anomalous skin effect, the  $R_{\text{pl}}(n_e)$  dependence is close to that obtained for media with a strong spatial dispersion [42, 45]. By and large, the nonmonotonic variation of the equivalent resistance as a function of plasma density is attributable to the competition between two factors: on the one hand, the RF-power absorption increases with a rise in the electron concentration and, on the other hand, the skin-layer depth determining the width of the domain of RF-power absorption decreases with  $n_e$ .

The theoretical model of the plasma source [42, 45] excited by a helical antenna located on its upper end surface predicts that the equivalent plasma resistance is independent of the plasma source length, provided that the skin-layer depth is



**Figure 2.** Dependence of the equivalent plasma resistance  $R_{pl}$  on the RF power  $R_{pl}$  absorbed by the plasma in the plasma excitation by helical antennas located on the lateral and end surfaces of the plasma source. Data of Aleksandrov et al. [46] (argon, 2 mTorr pressure) for  $R = 7.5$  cm with an ‘upper’ antenna for  $L = 10$  cm ( $\square$ ),  $L = 15$  cm ( $\circ$ ),  $L = 20$  cm ( $\blacktriangle$ ) and with a ‘side’ antenna for  $L = 10$  cm ( $\blacktriangledown$ ) and  $L = 20$  cm ( $\blacksquare$ ); analogous data for  $R = 11$  cm with an ‘upper’ antenna for  $L = 20$  cm ( $*$ ) and with a ‘side’ antenna for  $L = 20$  cm ( $\times$ ); 1 — data of Godyak et al. [47] (argon, 1 mTorr pressure, ‘upper antenna’,  $R = 10$  cm). (b) Equivalent plasma resistance as a function of plasma density. The data were calculated for plane disk-shaped sources 7.5 and 11 cm in radius by the formulas derived in Refs [42, 45]. Curve 1 — calculation without the inclusion of electron–ion collisions, 2 — with the inclusion of collisions, 3–5 — with the inclusion of collisions at pressures of 2, 10, and 30 mTorr, respectively; circles — experimental data [46] for an argon pressure of 2 mTorr.

smaller than the plasma source length. This result is physically evident, because the RF-power absorption takes place within the skin layer. Under experimental conditions, the skin-layer depth is known to be smaller than the length of plasma sources, and therefore it comes as no surprise that the equivalent resistance of the plasma sources equipped with an upper end antenna is independent of their length. In contrast, when the antenna is located on the lateral surface of the source, increasing the source length, which is simultaneously accompanied by an increase in antenna length, widens the domain in which RF-power absorption occurs, i.e., lengthens the skin layer. That is why the equivalent plasma resistance increases with source length in the case of a side antenna (Fig. 2a).

Experiments and calculations revealed that the absolute values of equivalent plasma resistance are not large at low pressures. Increasing the pressure of the working gas results in a substantial rise in equivalent resistance. This effect has been repeatedly noted in theoretical and experimental works [40, 42, 46–48]. The physical reason for the rise in the capability of

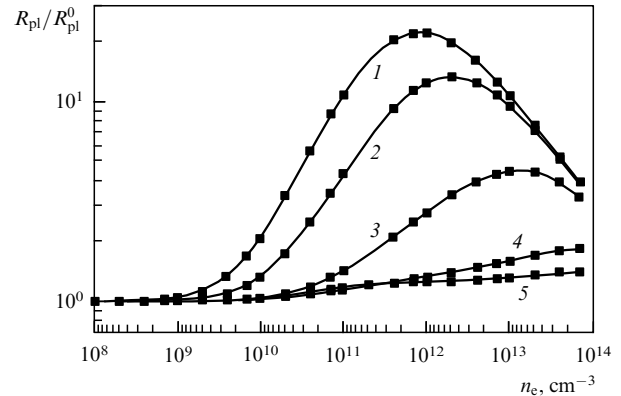


**Figure 3.** Ratio between the equivalent plasma resistance  $R_{pl}$ , which was calculated with the inclusion of collisional and collisionless absorption mechanisms, and the equivalent resistance  $R_{pl}^0$ , which was calculated only with the inclusion of collisions, as a function of plasma density. The calculations were made for plane disk-shaped plasma sources of radius 10 cm for a neutral gas pressure of 0.3 mTorr (1), 1 mTorr (2), 10 mTorr (3), 100 mTorr (4), and 300 mTorr (5).

plasma to absorb RF power with increasing pressure lies with the mechanism of RF-power absorption. Referring to Fig. 2b, the Cherenkov dissipation mechanism prevails for the lowest of the pressures considered, namely,  $p = 0.1$  mTorr. Electron–atom collisions can hardly affect the equivalent plasma resistance, while electron–ion collisions are responsible for only a minor increase in equivalent resistance for  $n_e > 3 \times 10^{11}$   $\text{cm}^{-3}$ . Raising the pressure, i.e., the electron–atom collision frequency, leads to an increase in the equivalent resistance, because the part played by the collisional mechanism of RF-power absorption becomes bigger. This is evident from Fig. 3 which depicts the ratio of the equivalent plasma resistance calculated with the inclusion of collisional and collisionless absorption mechanisms to the equivalent resistance calculated only with the inclusion of collisions.

### 3.4 Inductive discharge with an external magnetic field

Figure 4a displays the experimental dependences of the equivalent plasma resistance on the magnetic field induction, which were obtained for a fixed power deposited into the plasma [46]. In these experiments, use was made of plasma sources equipped with helical antennas located on their lateral and end surfaces, as well as with Nagoya III antennas. For an operating frequency of 13.56 MHz, the magnetic field intensity range  $B \approx 0.4–1$  mT corresponds to ECR conditions, and the range  $B > 1$  mT to the conditions of helicon and Trivelpiece–Gold wave excitation [41, 44].

The equivalent plasma resistance in the absence of a magnetic field at low pressures of the working gas ( $p \leq 5$  mTorr) is substantially lower than in the ‘helicon’ range. The  $R_{pl}$  values obtained for the ECR range occupy an intermediate position, with the equivalent resistance enhancing monotonically with a rise in the magnetic field induction. The ‘helicon’ range is characterized by a nonmonotonic dependence of the equivalent resistance on the magnetic field intensity, the nonmonotonicity of  $R_{pl}(B)$  for the end helical antenna and the Nagoya III antenna being pronounced much stronger than for the side helical antenna. The position and number of the local maxima of the  $R_{pl}(B)$  curve depend on the RF-power deposition, the length and radius of the plasma source, the kind of gas, and its pressure.

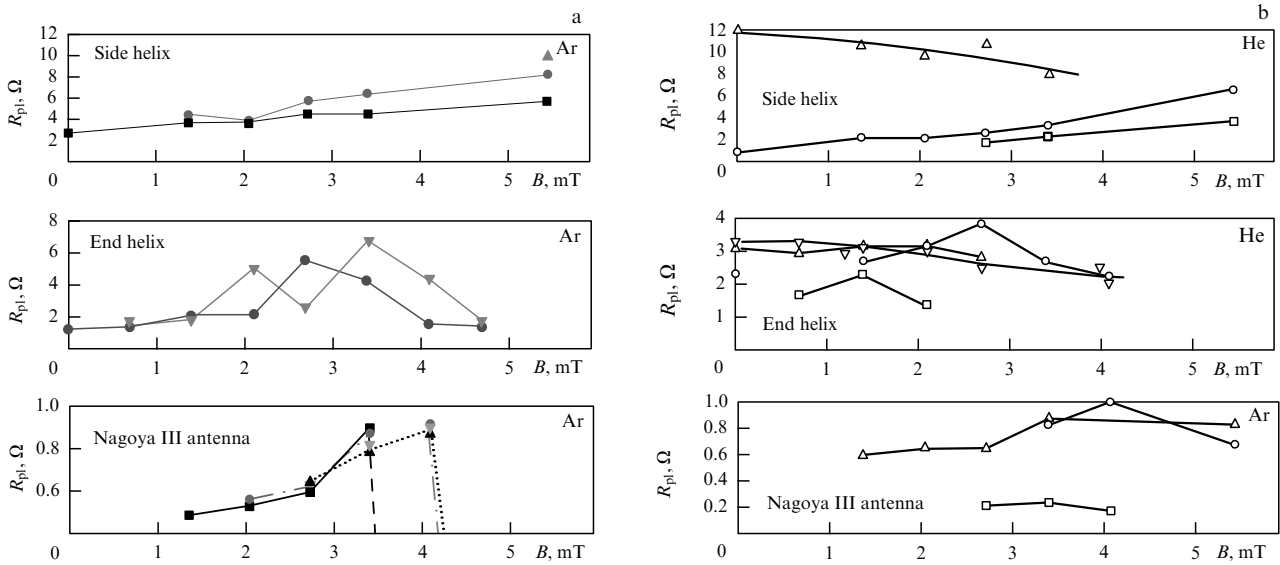


**Figure 4.** Dependences of the equivalent plasma resistance on the induction of an external magnetic field (a) for different powers deposited into the argon plasma at a pressure of 5 mTorr ( $R = 7.5$  cm,  $L = 20$  cm): 100 W (squares), 150 W (circles), 200 and 250 W (triangles with vertexes pointing up and down, respectively) with dashed lines indicating the discharge disruption, and (b) for different pressures of the inert gas ( $R = 7.5$  cm,  $L = 20$  cm,  $P_{pl} = 250$  W): 2 mTorr (squares), 5 mTorr (circles), 10 and 100 mTorr (triangles with vertexes pointing up and down, respectively).

Increasing the value of deposited power, i.e., the electron concentration  $n_e$ , leads to a rise in equivalent resistance and a shift of the main peak of the  $R_{pl}(B)$  function towards stronger magnetic fields, and in some cases gives rise to additional local maxima. A similar effect is also observed with an increase in the plasma source length [46].

As is evident from Fig. 4b, increasing the pressure in the 2–5 mTorr range does not lead to appreciable changes in the character of the  $R_{pl}(B)$  dependence. At pressures exceeding 10 mTorr, however, the nonmonotone behavior of the dependence of the equivalent resistance on the magnetic field intensity is no longer exhibited, and the absolute values of the equivalent resistance decrease and become smaller than the values obtained without the magnetic field.

The physical mechanisms of RF-power absorption by inductive discharge plasmas under ECR conditions, as well as the helicon and Trivelpiece–Gold wave excitation conditions, were analyzed in many theoretical papers [26–29, 33–37, 41, 44–46]. An analytical treatment of the helicon and Trivelpiece–Gold wave excitation problem in the general case presents serious difficulties, because it is required to describe two coupled waves. It should be recalled that a helicon represents a fast transverse wave, and a TG wave is a slow longitudinal wave. Helicons and TG waves turn out to be independent only in the case of a spatially unbounded plasma in which they are the oscillation eigenmodes of a magnetized plasma. For a bounded cylindrical plasma source, the problem allows only a numerical solution. However, the main features of the physical RF-power absorption mechanism for  $B > 1$  mT may be illustrated by means of the helicon approximation developed in Refs [44, 45], which describes wave excitation in the plasma subject to the following inequalities

$$\frac{c^2 k^2}{\omega_{Le}^2} \ll 1, \quad \frac{\omega}{\Omega_e} < \frac{\omega^2}{c^2 k_z^2} \varepsilon_{\perp} \approx \frac{\omega_{Le}^2 \omega^2}{\Omega_e^2 c^2 k_z^2} \ll 1. \quad (11)$$

Here,  $\omega$  is the field frequency,  $k_z \sim 1/L$  and  $k_{\perp} \sim 1/R$  are the longitudinal and transverse components of the wave vector,  $\Omega_e$  and  $\omega_{Le}$  are the cyclotron and Langmuir frequencies,  $k^2 = k_z^2 + k_{\perp}^2$ ,  $k_z = \pi n/L$ ,  $k_{\perp} = \mu_n/R$ ,  $n = 1, 2, 3, \dots$ , and  $\mu_n$  are the roots of the Bessel function.

In the helicon approximation, i.e., in the limit of sufficiently dense plasma, it is possible to uncouple the system of Maxwell equations for the RF fields excited in the plasma by the azimuthal current with an amplitude of  $I_0$ , which is carried by the antenna located on the lateral surface of the plasma source:

$$\begin{aligned} \frac{\partial}{\partial r} \frac{1}{r} \frac{\partial}{\partial r} r E_{\phi} - \alpha^2 E_{\phi} - \beta \frac{\omega}{c} \frac{\partial}{\partial r} E_z &= 0, \\ \frac{1}{r} \frac{\partial}{\partial r} r \frac{\partial}{\partial r} E_z - \tilde{k}_z^2 \frac{\varepsilon_{\parallel}}{\varepsilon_{\perp}} E_z &= k_z \frac{g}{\varepsilon_{\perp}} \frac{1}{r} \frac{\partial}{\partial r} r E_{\phi}, \end{aligned} \quad (12)$$

where

$$\tilde{k}_z^2 = k_z^2 - \frac{\omega^2}{c^2} \varepsilon_{\perp}, \quad \alpha^2 = \tilde{k}_z^2 - \frac{\omega^4 g^2}{c^4 k_z^2}, \quad \beta = \frac{\omega}{c} g \frac{k_z}{k_z^2}.$$

The boundary conditions have the form

$$E_{\phi}(z)|_{z=0} = 0, \quad \left. \frac{\partial E_{\phi}}{\partial z} \right|_{z=0} = 4\pi i \frac{\omega}{c^2 R} q I_0. \quad (13)$$

When inequalities (11) are satisfied, the last term on the left-hand side of the first of Eqns (12), which contains the longitudinal component of the electric field, may be neglected. Then, the first equation subject to the boundary condition permits calculating the azimuthal electric field of the helicon. We omit mathematical calculations, which are given in Refs [44, 45], and consider the dispersion relation for the helicons:

$$k_1 J_1'(k_1 R) K_1(k_z R) - k_z J_1(k_1 R) K_1'(k_z R) = 0, \quad (14)$$

where  $J$  and  $K$  are the Bessel and MacDonald functions.

For the typical dimensions of a plasma source,  $L \geq 10$  cm and  $R \leq 5$  cm, to a good approximation the solution of Eqn (14) is expressed as

$$k_1^2 R^2 \approx \pi^2 \left( n + \frac{1}{2} \right)^2, \quad \text{where } n = 1, 2, 3, \dots \quad (15)$$

Therefore, the excitation of helicons in the plasma is inherently resonant, and the resonance values of the magnetic field intensity (or the plasma density) can be found from the relationship

$$\frac{\omega^2 \omega_{Le}^2 R^2}{\Omega_c^2 c^2 k_z^2} \approx \frac{\pi^2 R^2}{L^2} + \pi^2 \left( n + \frac{1}{2} \right)^2. \quad (16)$$

In the excitation of bulk helicon waves in an elongated plasma source, the fields  $E_\phi^h$  and  $E_r^h$  become rather strong at resonance owing to the weak energy dissipation of the helicon field in the plasma. This, in turn, has the result that the helicon field, the field  $E_\phi^h$  in particular, comes to be the source of excitation of the potential field of the TG wave in the plasma. We note that the second equation of system (12) is basically the differential equation of oscillations under a driving force. As noted by Aleksandrov et al. [45], the TG-wave resonance, in principle, is also possible along with the helicon resonance described by dispersion relation (14). However, under conditions (11), i.e., in the framework of the helicon approximation, the TG-wave resonance proves to be impossible [45].

The total electric fields in the plasma are the sum of the helicon and potential fields of the TG wave:

$$E_z = E_z^L, \quad E_r = E_r^h + E_r^L \approx E_r^h, \quad E_\phi = E_\phi^h. \quad (17)$$

When substituting the expressions for the fields into the equation for the power absorbed by the plasma, it was found in Ref. [45] that under the conditions involved the helicon wave is only weakly absorbed in the plasma (due to the smallness of  $\text{Im}g$ ) and that the TG-wave field, by contrast, experiences a rather strong dissipation and heats the plasma.

Therefore, from the approximation employed it follows that an antenna with an azimuthal current  $j_\phi$  in a dense plasma resonantly excites a helicon field which is weakly absorbed by the plasma. When a weak coupling to the TG wave is taken into account, the helicon field in the magnetized plasma becomes a source of excitation of the potential TG wave which is strongly absorbed by the plasma.

Numerical simulations performed generally in the framework of the hydrodynamic model of a low-pressure RF inductive plasma source confirmed the above conclusions [41, 45] about the mechanism of RF-power absorption by the plasma. Figure 5a shows the typical dependences of  $R_{pl}$  on the magnitude of the magnetic field in the helicon domain, which were calculated for an argon pressure of 1 mTorr and different values of the plasma density. One can see that the  $R_{pl}$  functions exhibit a succession of local peaks which correspond to the conditions of resonance excitation of helicons and TG waves. Mathematical modeling makes it possible to separately analyze the contributions of the helicons and the TG waves to RF-power absorption by the plasma. Shown in Figs 5b,c is the equivalent plasma resistance calculated proceeding from only the RF helicon fields and only the TG wave fields. Referring to Figs 5b, c, the

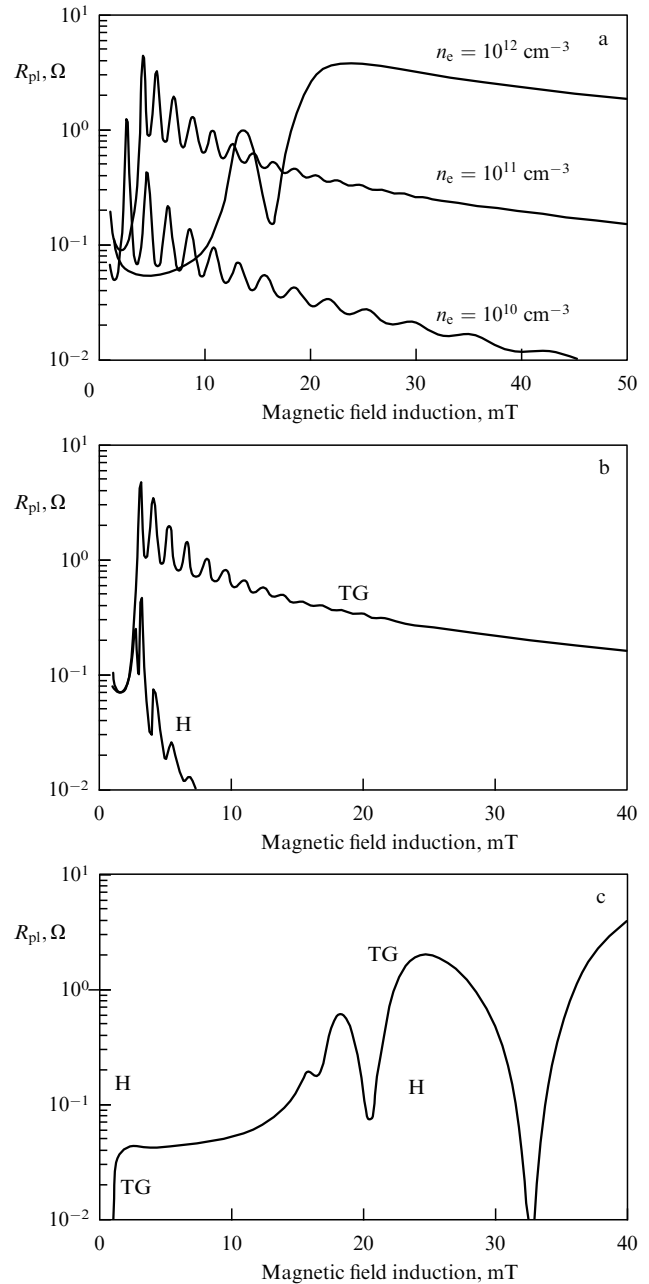


**Figure 5.** Equivalent plasma resistance as a function of the magnetic field induction calculated for (a) electron concentrations of  $10^{10}$ ,  $10^{11}$ , and  $10^{12}$   $\text{cm}^{-3}$  for a plasma source with  $R = 5$  cm,  $L = 20$  cm; (b, c) analogous dependences for (b)  $n_e = 10^{11}$   $\text{cm}^{-3}$ , and (c)  $n_e = 3 \times 10^{12}$   $\text{cm}^{-3}$  ( $p = 1$  mTorr) for a plasma source with  $R = 5$  cm,  $L = 15$  cm with the inclusion of only the Trivelpiece–Gold wave (TG) and with the inclusion of only the helicon (H).

TG wave makes the main contribution to absorption at electron concentrations of  $10^{11}$   $\text{cm}^{-3}$  and below. Since the TG wave represents a quasilongitudinal wave, its absorption is primarily determined by the collisionless Cherenkov mechanism. At higher electron concentrations (Figs 5b, c), the contribution of helicons to absorption is comparable to the TG-wave contribution in the region of magnetic field intensities not exceeding 200 G. In the region of stronger magnetic fields, the TG-wave absorption prevails everywhere, with the exception of narrow regions in which the TG-wave amplitude has local minima.

The behavior of equivalent plasma resistance with increasing magnetic field intensity at a plasma density of  $10^{11} \text{ cm}^{-3}$  is substantially different from that obtained for  $n_e = 3 \times 10^{12} \text{ cm}^{-3}$ . This is due to the effect of electron–ion collisions. By and large, the increase in collision frequency caused by an increase in the gas pressure or a rise in electron–ion collision frequency with plasma density has the effect that the dependence of electric field amplitudes on the magnetic field induction smooths out. Furthermore, the TG-wave amplitude lowers with increasing collision frequency and the bulk wave turns into a surface wave [41]. For this reason, the equivalent plasma resistance lowers. It is noteworthy that the helicon amplitude and helicon penetration depth into the plasma do not change with increasing pressure.

One can see from Fig. 5a that the main peak in the dependence of the equivalent resistance on the magnetic field induction shifts towards stronger magnetic fields with an increase in the plasma density (or the power deposited into the plasma). This signifies that  $R_{pl}$  as a function of electron concentration for a fixed induction  $B_0$  is a decreasing function in the region of high electron concentrations. This result is physically evident, because the amplitudes of the electric fields become lower and their penetration into the plasma sharply deteriorates on exiting the resonance with an increase in plasma density. The higher the magnetic field induction, the higher is the critical density of the plasma, upon exceeding which a fall in equivalent plasma resistance occurs.

In concluding this section we list the main features of the behavior of equivalent plasma resistance:

- 1)  $R_{pl}$  depends nonmonotonically on the plasma density;  $R_{pl}$  increases with  $n_e$  in the range of low electron concentrations; in the region of high electron concentrations, the capacity of the plasma for power absorption lowers due to the impairment of RF-field penetration into the plasma;
- 2) in the absence of a magnetic field, a significant part in RF-power absorption is played by the collisional mechanism, and therefore increasing the gas pressure and the electron concentration leads to an increase in  $R_{pl}$ ;
- 3) in the helicon domain, the behavior of  $R_{pl}$  under changes in the magnetic field intensity at low pressures is strongly nonmonotonic and resonant in character;
- 4) in the presence of a magnetic field, a significant part is played by the collisionless Cherenkov mechanism in the domains of resonance RF-power absorption, and therefore raising the pressure leads to a decrease in  $R_{pl}$ .

#### 4. Properties of a low-pressure radio-frequency inductive discharge operating in the $R_{pl} \leq R_{ant}$ regime

The results presented in Section 3 imply that the equivalent plasma resistance changes significantly under variations in the plasma density and the conditions of discharge maintenance, in particular, under variations in the pressure and the intensity of an external magnetic field. This should give rise to emerging properties (not always desirable) in the behavior of an RF inductive discharge in plasma sources operating in the  $R_{pl} \leq R_{ant}$  regime. Below, we consider the results of experiments staged with the aim of revealing these properties [46] and the data of numerical discharge simulation, which elucidate the physics of the observed effects. A self-consistent model of the RF inductive source was outlined in Refs [41, 46]. The results given below were obtained assuming a linear dependence of the electron concentration on the power

deposited into the plasma [41, 46]:

$$n_e = \alpha P_{pl}. \quad (18)$$

We begin our consideration with the dependence of plasma parameters on the RF-generator power.

#### 4.1 Dependence of plasma parameters on the radio-frequency plasma source power

Figure 6a demonstrates typical dependences of the intensity of plasma glow on the RF-generator power. In accordance with modern notions [38, 49, 50], the run of the curve is interpreted as follows: the discharge is ignited and operates at a low power in the capacitive mode, then, as the generator power increases, some critical value of the antenna current [38] is reached and conditions emerge for a discharge transition to the inductive mode. As this takes place, the electron concentration and, hence, the plasma glow intensity rise sharply. Subsequently, the discharge operates in the inductive mode with a high electron concentration.

Simulation data (Figs 6b, c) permit the physics of the processes to be substantially elucidated. The solutions to the system of equations, which correspond to possible discharge modes, exist for a generator power exceeding some threshold value  $P_{min}$ , which depends both on the conditions of discharge maintenance and on the antenna resistance. For a low antenna resistance, the discharge abruptly passes to the mode with a high electron concentration (hereinafter — the high mode) as soon as the threshold power is exceeded. However, as the antenna resistance increases, solutions emerge indicating the possibility of discharge occurrence in the mode with a low electron concentration (hereinafter — the low mode). When the discharge operates in the low mode, the bulk of generator power is lost in the antenna, and the power deposited to the discharge maintains only a low electron concentration which is close in magnitude to the electron concentration existing in the RF capacitive discharge. Raising the RF-generator power leads to a rise in plasma density and, accordingly, in equivalent plasma resistance. When the power deposited into the discharge becomes significant, a ‘chain reaction’ occurs: the increase in the equivalent plasma resistance and, hence,  $P_{pl}$  results in an increase in  $n_e$ , which in turn leads to an increase in  $R_{pl}$  and  $P_{pl}$ . These processes are responsible for an abrupt low-to-high mode transition of the discharge. The electron concentration in the high discharge mode is rather high — on the order of  $10^{11} \text{ cm}^{-3}$ . As shown in Section 3, in the region of relatively high electron concentrations — on the order of  $10^{11} \text{ cm}^{-3}$  — the equivalent resistance as a function of plasma density is observed to become saturated. That is why the growth of plasma density in the high discharge mode with increasing generator power moderates and in some cases saturation of the plasma density occurs. This limits the possibility of controlling discharge parameters in the mode with a high electron concentration.

It is well known that in some cases a hysteresis occurs in the dependence of plasma parameters on the RF-generator power in the domain of low-to-high discharge mode transition. The data of numerical simulations [41, 46] (Fig. 6c) suggest that there sometimes occurs an ambiguity of solutions in the domain of transition between inductive discharge modes, which may underlie the experimentally examined hysteresis. To analyze the prerequisites for the emergence of multiple solutions, we perform simple algebraic transforma-

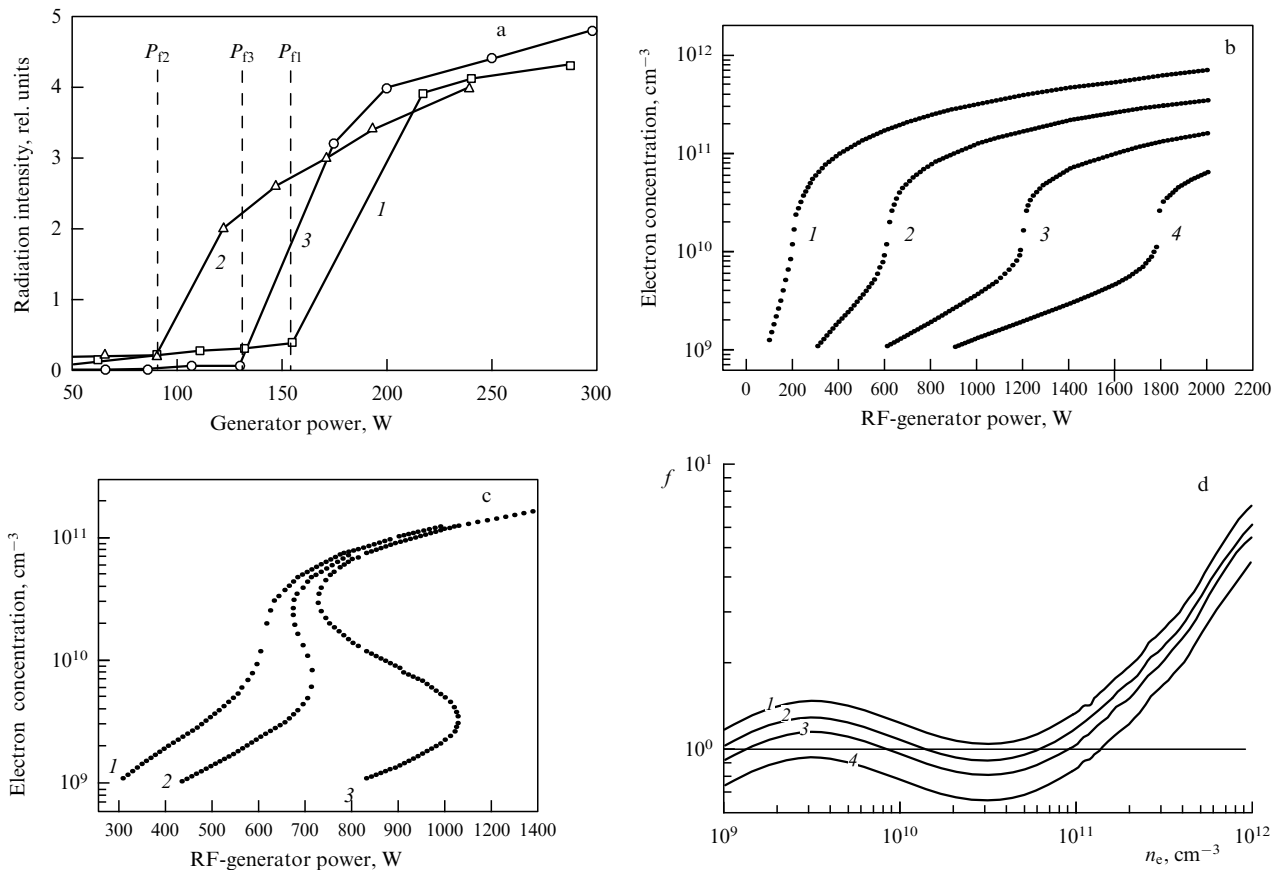


**Figure 6.** (a) Plasma glow intensity as a function of the power of an RF generator with an end helical antenna: 1 — a purely inductive discharge; 2 — an independent capacitive channel, the power of the RF generator that feeds the capacitive channel is 100 W, and 3 — a hybrid discharge;  $P_{f1}$ ,  $P_{f2}$ , and  $P_{f3}$  are the threshold powers at which the inductive discharge experiences a transition from the mode with a low glow intensity to the mode with a high glow intensity upon increasing the generator power. (b, c) Electron concentration as a function of RF-generator power in the inductive discharge in a plasma source of radius 5 cm without a magnetic field. Solution to the self-consistent problem (b) for different antenna resistances: 0.3  $\Omega$  (1), 1  $\Omega$  (2), 2  $\Omega$  (3), and 3  $\Omega$  (4) for a gas pressure of 0.3 mTorr, and (c) for different neutral gas pressures: 0.3 mTorr (1), 0.2 mTorr (2), and 0.1 mTorr (3) for an antenna resistance of 0.5  $\Omega$ . (d) Graphic solution of Eqn (19) at RF-generator power levels of 700 W (curve 1), 800 W (curve 2), 900 W (curve 3), and 1100 W (curve 4).

tions and reduce the system of equations (1), (2), (18) to a single equation

$$1 = \frac{\alpha n_e (1 + R_{ant}/P_{pl})}{P_{gen}} \equiv f(n_e). \quad (19)$$

It is evident that the entire generator power for  $R_{pl} \gg R_{ant}$  is deposited into the plasma and the electron concentration varies in proportion to the RF-generator power. We emphasize that the relation between  $n_e$  and  $P_{gen}$  remains unambiguous in this case. In the opposite case of  $R_{pl} < R_{ant}$ , solutions may also emerge, and there may be several solutions if the dependence of  $R_{pl}$  on the electron concentration is nonmonotonic in the  $R_{pl} < R_{ant}$  region.

Figure 6d depicts the function  $f(n_e)$  calculated for a low-pressure inductive discharge in the absence of a magnetic field. As evident from Fig. 6d, for an RF-generator power of 700 W the inequality  $f(n_e) > 1$  is satisfied throughout the electron concentration range considered. This signifies that no solutions exist and an RF inductive discharge cannot occur under the generator power involved. For an RF-generator power of 800–900 W, an RF inductive discharge may occur, but the equivalent plasma resistance corresponding to the highest possible electron concentration is low in comparison with the antenna resistance and is nonmonoto-

nically dependent on the electron concentration. This underlies the nonmonotonic behavior of  $f(n_e)$  as a function of  $n_e$  and the emergence of two or three solutions to the discharge-describing system of equations for an RF-generator power of 800–900 W. The further increase in power eliminates multi-valuedness and gives rise to the unique value of the plasma density satisfying the system of equations (1), (2), (18).

Let us consider the effect of an external magnetic field on the hysteresis. Figure 7 illustrates the measured plasma glow intensity  $J$  as a function of RF-generator power  $P_{gen}$  for fixed values of the magnetic field induction. Typical  $J(P_{gen})$  dependences at magnetic field intensities below 2 mT are similar to the dependences obtained in the absence of a magnetic field. The discharge is ignited in the low mode, and as the RF-generator power increases an abrupt transition to the high discharge mode occurs. Upon lowering the RF-generator power, the high-to-low mode jump takes place at a value of  $P_{gen} = P_b$ , which is equal to the value of  $P_{gen} = P_f$  at which the low-to-high mode jump occurs under variations in the RF-generator power  $P_f$ . The situation is changed when the magnetic field intensity is above 1 mT. In this case, a hysteresis emerges and  $P_b$  turns out to be lower than  $P_f$ , with the difference between  $P_b$  and  $P_f$  increasing with an increase in the magnetic field intensity. Also noteworthy is the fact that the transition region shifts to the higher-power region with

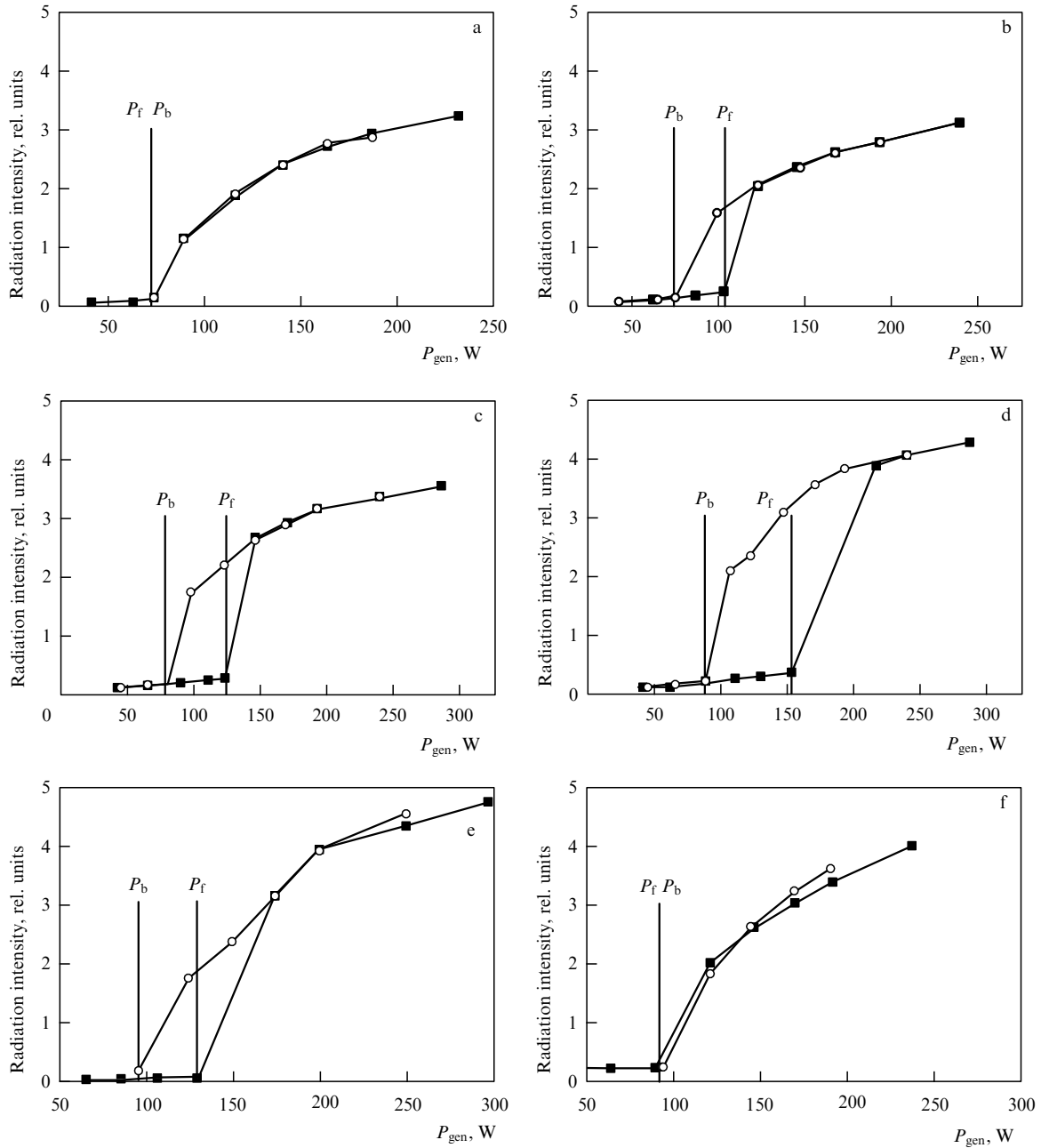


**Figure 7.** Plasma glow intensity as a function of RF-generator power upon increasing (squares) and decreasing (circles) power in magnetic fields (a) 1 mT, (b) 1.2 mT, (c) 1.3 mT, and (d–f) 1.4 mT. (a–d) Inductive discharge, (e) hybrid discharge, (f) discharge with independent inductive and capacitive channels; the power of the RF plasma source that feeds the capacitive channel is 100 W. The argon pressure is equal to 2 mTorr.

increasing magnetic field intensity. In particular, in a magnetic field exceeding 1.4 mT the highest RF-generator power  $P_{\text{gen}} = 300$  W employed in the work turns out to be insufficient for the low-to-high discharge mode transition.

Qualitatively similar features are also observed in the numerical simulation of the RF inductive discharge in an external magnetic field [41]. As for a discharge without a magnetic field, the inductive discharge is only possible when the power exceeds the threshold value  $P_{\text{min}}$ . Furthermore, simulations show that, in addition to the above-listed factors that affect the value of  $P_{\text{min}}$ , there appears a dependence on the magnetic field induction  $B$ , as well. One can see from Fig. 8 that in moderate magnetic fields,  $B \leq 2$  mT, the increasing of the RF-generator power leads to a sharp rise in electron concentration (to a transition to the high mode) as soon as

the conditions for the existence of solutions to the system of discharge equations are fulfilled, with a one-to-one correspondence between the plasma density and the RF-generator power. The picture somewhat changes with increasing the magnetic field intensity. In the region of a sharp rise in plasma density there emerges the second solution which corresponds to the low discharge mode. Increasing the induction of an external magnetic field gives rise to multivaluedness of solutions and leads to the broadening of the RF-generator power range in which several discharge modes may exist. The reason for the emergence of the multivaluedness of solutions lies with the nonmonotonic variation (oscillating behavior) of the equivalent plasma resistance as a function of electron concentration, which stems from the resonance nature of helicon and TG wave excitation in the discharge (see Ref. [46]).

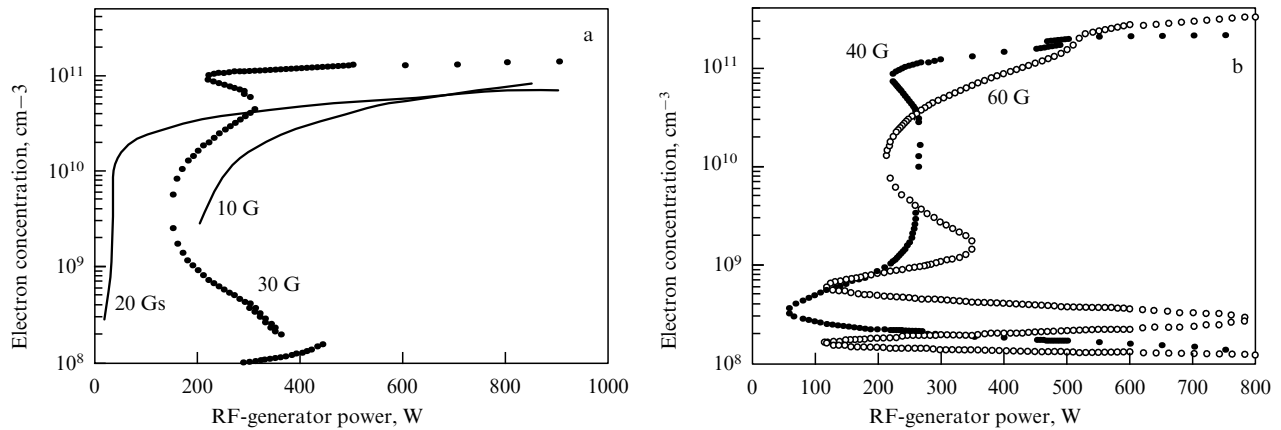


**Figure 8.** Electron concentration as a function of RF-generator power for different magnitudes of the magnetic field.

Therefore, the solutions to the self-consistent discharge problem showed that the typical form of the dependence of the plasma density on the RF-generator power is due to the self-consistent power redistribution between the antenna and the plasma [41, 46]. The RF inductive discharge may exist in two modes: with a low and high electron concentration. In the low mode, the bulk of RF-generator power is lost in the antenna, while in the high mode a significant fraction of the power  $P_{\text{gen}}$  is released in the plasma. Observed in the high discharge mode is a moderation of the plasma density growth in connection with the saturation of equivalent plasma resistance as a function of  $n_e$  at electron concentrations on the order of  $10^{11} \text{ cm}^{-3}$ . In the transition region between the modes, an abrupt rise in plasma density occurs and a hysteresis may emerge. The hysteresis occurs when the equivalent plasma resistance, first, is small in comparison with the antenna resistance and, second, depends nonmonotonically on the plasma density.

#### 4.2 Dependence of plasma parameters on the external magnetic field

The experiments presented in this section were performed with an end spiral antenna with an effective resistance of  $3.6 \Omega$  [46], which enabled realizing a regime with  $R_{\text{pl}} \leq R_{\text{ant}}$  over a wide range of magnetic field intensities and RF-generator powers.

Figures 9a, b exhibit the variation in the electron concentration and effective electron temperature at the center of the plasma source upon varying the magnitude of the magnetic field. The load was matched to the RF plasma source for each magnitude of the magnetic field considered, so that the value of RF power which the generator delivered to the external circuit remained constant. One can see that the electron concentration is low in the absence of a magnetic field. Raising the magnetic field induction  $B$  leads to a sharp rise in plasma density; then, when the magnetic field intensity exceeds some value  $B_{\text{max}}$ , the electron concentration lowers, and on reaching some critical value  $B_{\text{cr}}$  of the magnetic field induction the discharge disruption occurs. The variation in plasma density is simultaneously accompanied by the spatial redistribution of the plasma (Figs 9c, d). Strengthening the magnetic field leads initially to a total rise in electron concentration, especially in the central discharge regions. Next, prior to discharge disruption, the plasma density

lowers throughout the section and the peripheral discharge regions come to be most significant. Despite the substantial change in the electron concentration, the effective electron temperature depends only slightly on the magnetic field intensity and the RF-generator power. Increasing the RF-generator power and the working gas pressure has the effect that the discharge disruptions shift towards stronger magnetic fields, i.e., the critical induction  $B_{\text{cr}}$  increases. In some cases, increasing the RF-generator power gives rise to a second and sometimes third local plasma density peak in the region of weaker magnetic fields. The existence domain of all the maxima is abruptly bounded from the side of strong magnetic fields.

It would be reasonable to assume that the power redistribution between the antenna and the plasma in accordance with formulas (1) and (2) is the cause of nonmonotonic plasma density variation upon altering the magnetic field induction. In this connection, the RF powers absorbed by the plasma at different magnitudes of magnetic fields [46] were determined in experiments with a purely inductive discharge on the basis of measurements of the current  $I_{\text{ant}}$  carried by the antenna as a function of the external magnetic field intensity. The measurements showed that the discharge ignition results in a small lowering of the current flowing through the antenna, and the further increase in the magnetic field intensity increases the difference between the currents carried by the antenna during discharge and in its absence. This is an indication that the fraction of RF-generator power absorbed by the plasma increases. Raising the magnetic field induction for  $B > B_{\text{max}}$  results in increasing the current carried by the antenna. Upon discharge disruption, the antenna current reverts to the values which took place prior to discharge ignition.

Figure 10 depicts the values of the RF power  $P_{\text{pl}}$  absorbed by the plasma, which were calculated proceeding from the measured  $I_{\text{ant}}$  values. Referring to Fig. 10, the power  $P_{\text{pl}}$  rises with increasing magnetic field induction up to the value  $B_{\text{max}}$ ; then, for  $B > B_{\text{max}}$ , the power lowers until it reaches values insufficient for maintaining the discharge. At this point, discharge disruption occurs.

The variation in power absorbed by the plasma with increasing magnetic field intensity should naturally be compared with the dynamics of electron concentration variations. As noted above, an increase in the magnetic field intensity is responsible for a redistribution of plasma

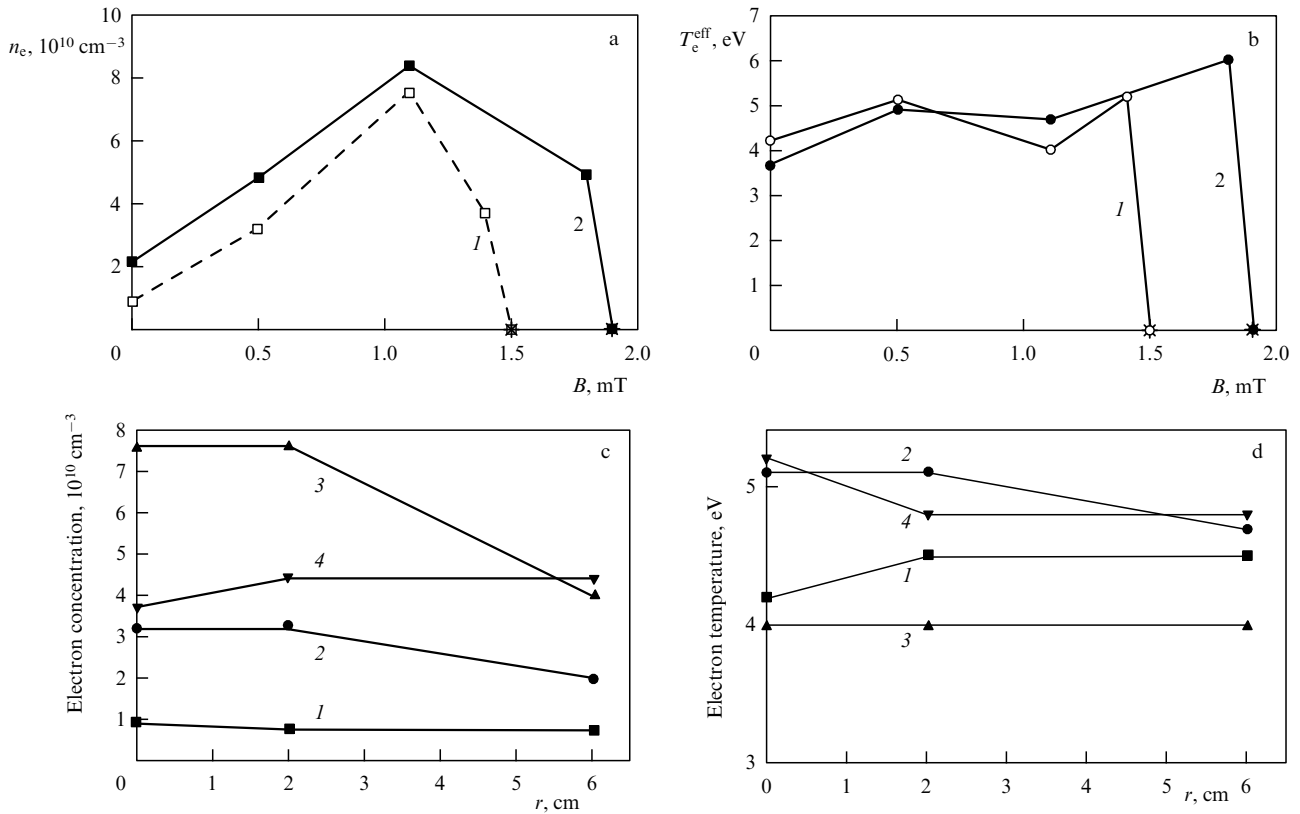
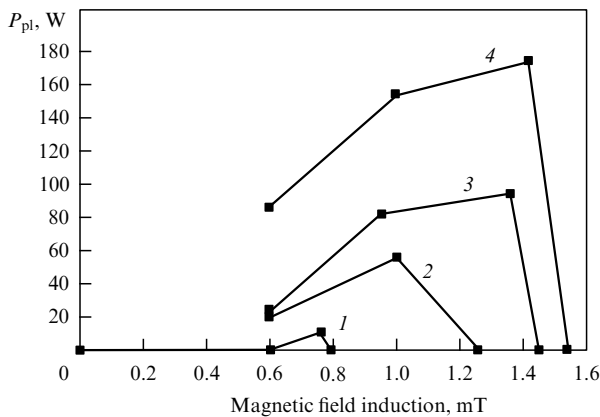


**Figure 9.** Electron concentration  $n_e$  (a) and effective electron temperature  $T_e^{\text{eff}}$  (b) as functions of an external magnetic field induction  $B$  for an RF-generator power of 150 W (1) and 200 W (2); the argon pressure was 2 mTorr, with an end antenna discharge. Dependences of  $n_e$  (c) and  $T_e^{\text{eff}}$  (d) on the distance  $r$  to the source axis are given for  $B = 0$  (1), 0.5 mT (2), 1.1 mT (3), and 1.4 mT (4); the discharge was ignited in a 15-cm-long plasma source of radius 7.5 cm; the RF-generator power equaled 150 W, and the argon pressure was 4 mTorr.

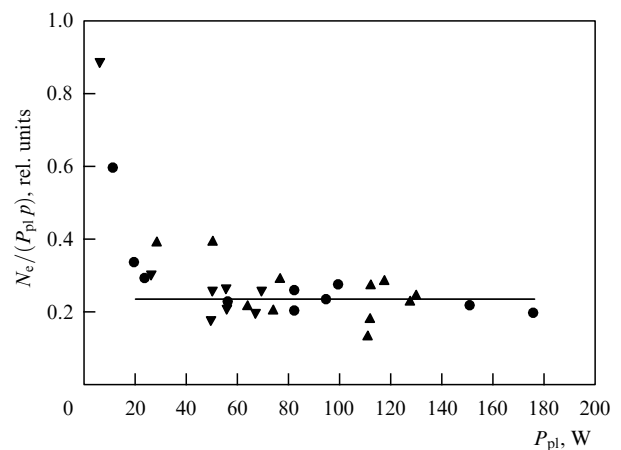
parameters over the source volume. In this case, the section-averaged values of the electron concentration  $N_e$  were used in the analysis in Ref. [46].

Figure 11 gives the experimental data of Ref. [46], presented as the dependence of  $N_e/(P_{\text{pl}}p)$  on the power absorbed by the plasma, where  $p$  is the argon pressure in the discharge chamber. With reference to Fig. 11, when the power deposited into the plasma exceeds 40 W, a straight line parallel to the abscissa fits, to within experimental error, all the data points. This signifies that the volume-

average electron concentration in the plasma of an RF inductive discharge is proportional to the power deposited into the plasma, while the peculiarities in the behavior of plasma density upon variations in the magnetic field intensity are due to the redistribution of RF-generator power between the active effective antenna resistance and the equivalent plasma resistance. The rise in the  $N_e/(P_{\text{pl}}p)$  ratio in the region of low ( $P_{\text{pl}} < 40$  W) powers released in the plasma is supposedly due to the existence of the capacitive discharge component.



**Figure 10.** Power deposited into the plasma as a function of the magnetic field induction for an RF-generator power of 100 W (1), 150 W (2), 200 W (3), and 300 W (4). The argon pressure was 2 mTorr. The discharge is driven by an end antenna.



**Figure 11.** Dependence of  $N_e/(P_{\text{pl}}p)$  on the power absorbed by the plasma.

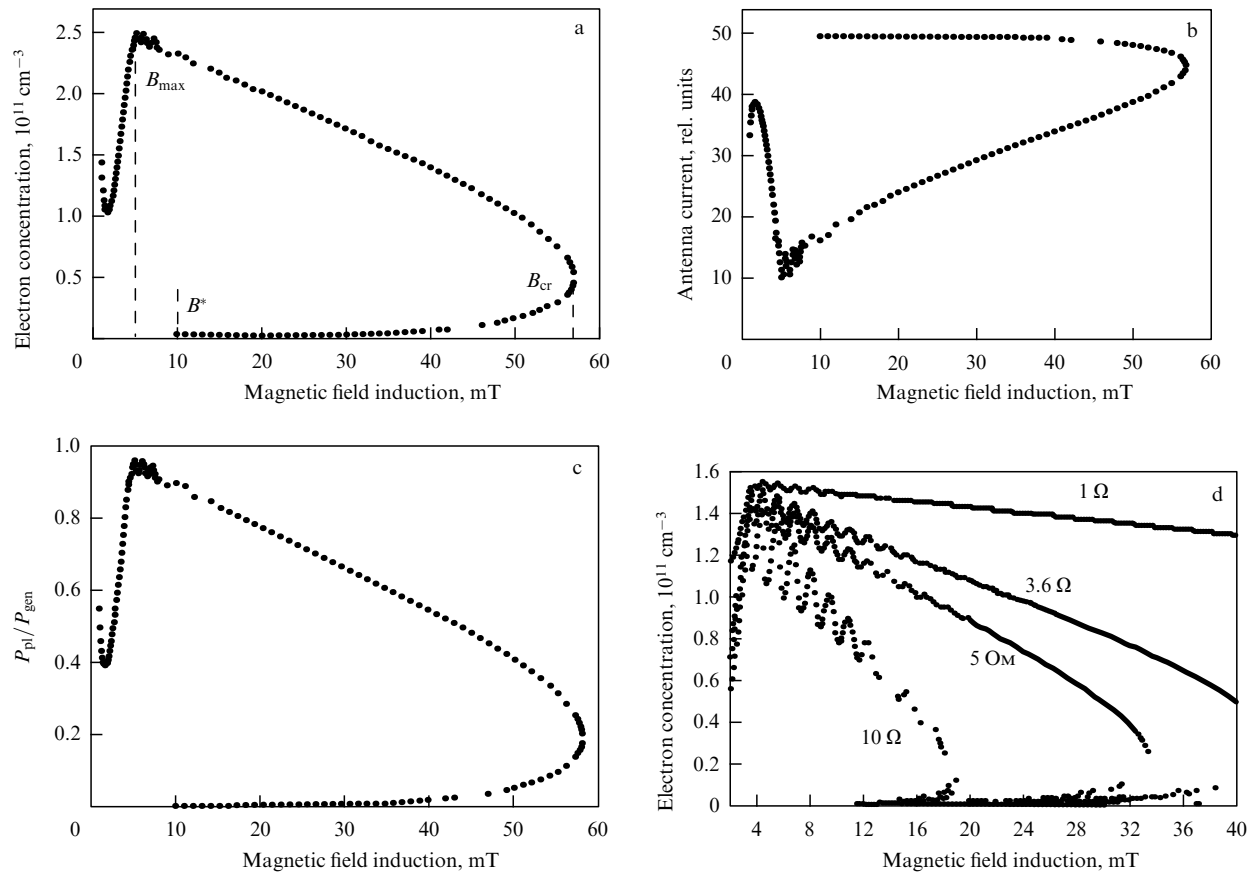


**Figure 12.** (a–c) Electron concentration, antenna current, and efficiency  $P_{pl}/P_{gen}$  of RF-power deposition into the plasma as functions of the magnetic field induction; the generator power amounts to 500 W, the antenna resistance is  $0.2 \Omega$ , the plasma source radius equals 5 cm, and the plasma source length is 15 cm. (d) Dependence of the electron concentration on the magnetic field induction for different antenna resistances.

To make more lucid the physical picture of the effects described above, we will consider the data of numerical simulations [41, 46]. Figures 12a–c depict the electron concentration, the antenna current, and the efficiency of power deposition into the plasma as functions of magnetic field induction  $B$  for a fixed RF-generator power. As in experiments, with strengthening magnetic field the antenna current initially decreases, and then, for  $B > B_{max}$ , begins to increase, and finally reverts to the values which it possessed in the absence of discharge. The power deposited into the plasma and the electron concentration increase with increasing the magnetic field induction up to a value of  $B = B_{max}$ , and decrease after that. The system of equations describing the discharge has no solutions for magnetic field inductions  $B > B_{cr}$ . Physically, this is an indication that the discharge cannot exist. The reason why there is no solution at large  $B$  values lies with a substantial lowering of the equivalent plasma resistance due to the impairment of RF-field penetration into the plasma and the lowering of the fraction of power absorbed by the plasma to values insufficient for discharge maintenance. Increasing the RF-generator power, which is accompanied by an increase in plasma density and equivalent resistance, as well as increasing the pressure, which in some cases leads to an increase in equivalent resistance in the region of strong magnetic fields, is accompanied by a shift in the right bound of the solution existence domain towards higher  $B$  [46].

The increase in antenna resistance (Fig. 12d) broadens the range of the magnetic field intensities in which  $R_{pl} \leq R_{ant}$ . We

note that in this case the dependence of plasma density on the magnetic field induction exhibits local peaks, their heights decreasing in the region of strong magnetic fields. As shown in Section 3, the dependence of  $R_{pl}$  on  $B$  for plasma sources of relatively long radius and length is characterized by the presence of several local maxima related to the positions of helicon and TG wave excitation resonances. Moving away from the resonance is accompanied by a sharp decrease in the equivalent resistance, the fraction of power absorbed by the plasma, and, accordingly, the plasma density. The drop in plasma density, in turn, lowers the equivalent resistance and the power deposited into the plasma. In this case, in the region of sharp  $R_{pl}$  lowering there occurs an abrupt decrease in the plasma density with an increase in the magnetic field intensity. A comparison of Fig. 12d with experimental data allows the conclusion that the abrupt plasma density steps observed in experiments are related to helicon and TG wave excitation resonances which manifest themselves in sharp variations in the plasma capacity for absorbing the RF power.

By and large, comparing the data of numerical simulations and experiments points to the conclusion that the behavior of the plasma density of an RF inductive discharge upon variations in the magnitude of an external magnetic field is determined by the self-consistent RF-power redistribution between the plasma and the external circuit, the redistribution being governed by the physical mechanisms of electric field penetration into the plasma and RF-power absorption.

The experimental data presented in the foregoing were obtained in Ref. [46] for a fixed generator power, with the magnetic field induction being increased from zero to the values  $B_{\text{fin}}$  exceeding the field inductions  $B$  at which discharge disruption was observed. In some cases, when the magnetic field induction was initially increased from 0 to  $B_{\text{fin}}$  and then lowered to 0, a hysteresis was observed in the plasma density as a function of the magnetic field induction. Measurements of the RF power absorbed by the plasma showed that two regimes are realized for the same RF-generator power for some magnetic fields: in one regime, practically all power is released in the external circuit and the plasma density is small, while in the other regime almost all power is absorbed by the plasma and the electron concentration is high.

Mathematical modeling [41, 46] (see Fig. 12) showed that in some cases there are several solution branches for the same values of external magnetic induction  $B$  and RF-generator power  $P_{\text{gen}}$ , i.e., several values of the electron concentration whereat a solution of the system of equations describing the discharge exists. Considered earlier was the solution branch with high electron concentrations; however, beginning from some value  $B^*$  there emerges a second equilibrium solution with plasma densities approximately an order of magnitude lower than the corresponding densities of the first solution. Clearly, the existence of several values of electron concentration for the same values of  $B$  and  $P_{\text{gen}}$  testifies to the possible occurrence of a hysteresis with increasing and decreasing external magnetic field induction.

Therefore, in the operation of an RF inductive discharge in the regime  $R_{\text{pl}} \leq R_{\text{ant}}$ , a self-consistent power redistribution occurs between the plasma and the active resistance of the external circuit, which manifests itself in the following:

- (1) the existence of two modes of an RF inductive discharge with strongly different values of the plasma density;
- (2) the occurrence of a hysteresis in passing from the low discharge mode to the high one and back, respectively, with increasing and decreasing external magnetic field induction;
- (3) saturation of the dependence of the plasma density on the RF-generator power in the high- $n_e$  region;
- (4) the boundedness, in the presence of external magnetic field, of the discharge existence domain from the side of strong magnetic fields;
- (5) the nonmonotonicity of the dependence of the plasma density on the external magnetic field induction.

## 5. Properties of a radio-frequency inductive discharge with a capacitive component

We now consider the effect of antenna–plasma capacitive coupling on discharge characteristics. To study the effect of the capacitive discharge component, capacitor plates were mounted on the outer lateral surface of the plasma source in addition to the helix located on the end surface in the experiments of Ref. [46] (Fig. 1c). This enabled a capacitive power input channel to be organized without changing the antenna–plasma inductive coupling. The capacitor was connected in two ways. In the first case, the antenna ends and the capacitor plates were connected to two independent RF plasma sources via individual matching systems. In this case, the RF power could be independently deposited via the inductive and capacitive channels. In the other case, the inductor and the capacitor were connected in parallel to a common RF plasma source to model the real inductive RF

discharge possessing a capacitive component (hereinafter, a hybrid RF discharge).

### 5.1 Dependence of plasma parameters on the radio-frequency plasma source power

Our consideration of the effect of the capacitive component on the parameters of an inductive discharge begins with the case of lacking a magnetic field. One can see from Fig. 6a that the existence of an independent capacitive channel lowers the critical power  $P_f$  at which the discharge passes into the mode with a high glow intensity and which is deposited via the inductive channel. The higher the fraction of RF power input via the capacitive channel, the lower the  $P_f$  value. Simultaneously with the lowering of  $P_f$ , the transition from the mode with a low glow intensity to the mode with a high intensity becomes smoother. The case of parallel antenna–capacitor connection leads to qualitatively the same results; however, the change in  $P_f$  is much more weakly pronounced.

In the presence of an external magnetic field, the occurrence of a capacitive component leads to changes not only in  $P_f$ , but also in  $P_b$  [46]. As is evident from Figs 7e, f, the difference between  $P_f$  and  $P_b$  is substantially smaller for a parallel antenna–capacitor connection than for a purely inductive discharge, and upon increasing the RF power delivered to the plasma via an independent capacitive channel, the difference between  $P_f$  and  $P_b$  tends to zero and the hysteresis vanishes. Therefore, the occurrence of a capacitive component leads to discharge stabilization and the disappearance of the hysteresis in the dependence of plasma parameters on the RF power and the magnetic field intensity.

We highlight one more significant result. When the antenna and the capacitor are connected in parallel, the lowering of antenna current in the high discharge mode does not exceed 10%, in comparison with the current for a purely inductive discharge under all the experimental conditions considered. The intensity of plasma glow in the high discharge mode also depends only slightly on the presence of the capacitive discharge component (Fig. 6a).

We now consider the results of numerical simulations of a discharge with an independent capacitive component, which

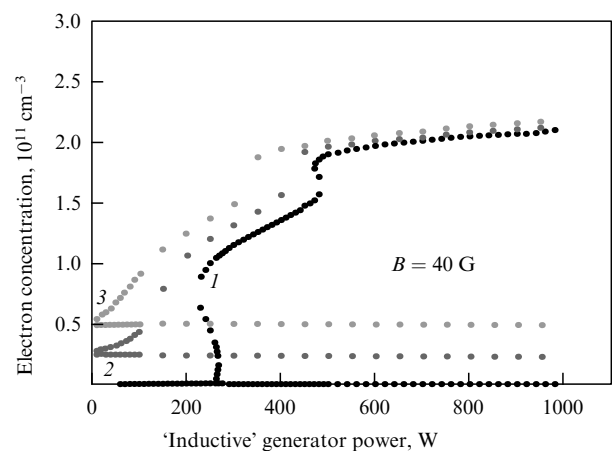


**Figure 13.** Electron concentration as a function of ‘inductive’ RF-generator power ( $B = 40$  G) for different values of ‘capacitive’ generator power: 1 — without the capacitive component, 2 — the capacitive component is equal to 50 W, and 3 — the capacitive component is equal to 100 W.

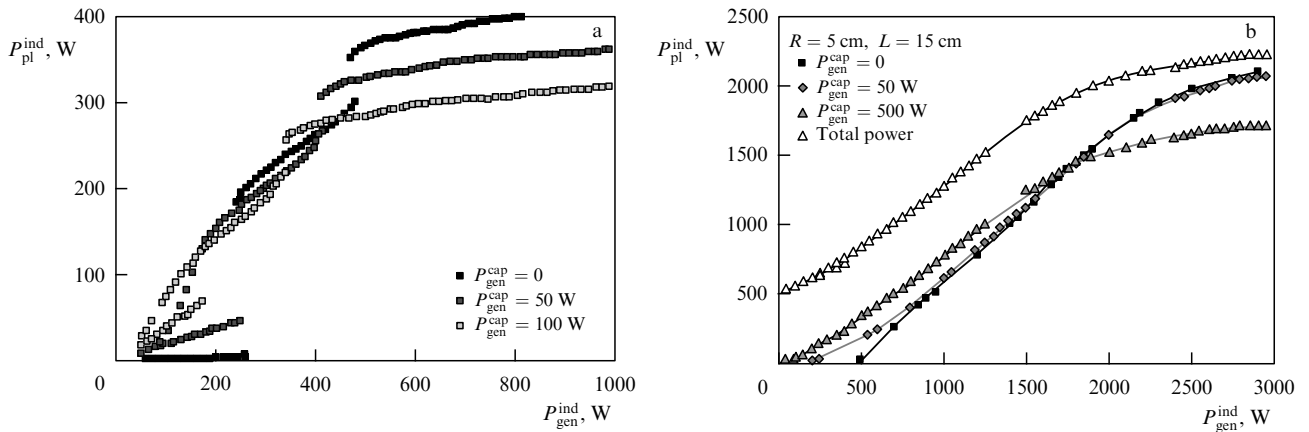


**Figure 14.** Power deposited into the plasma via the inductive channel and total power as functions of the ‘inductive’ RF-generator power for different values of the ‘capacitive’ generator power: (a)  $B = 40$  G, and (b)  $B = 150$  G.

permit elucidating the physical causes of the observed effects. Figure 13 shows the dependence of the RF-discharge plasma density  $n_e$  on the RF-generator power  $P_{gen}^{ind}$ , which feeds the inductive channel in a purely inductive discharge, including the case when the power is additionally deposited into the discharge via a capacitive channel. It is clear that in the presence of the capacitive channel the discharge may exist in modes with considerably different plasma densities. In the case of a high-density mode, the major part of the RF-generator power which feeds the inductive channel is deposited into the plasma. In the mode with a low electron concentration, practically all the power of the inductive generator goes to heat the antenna, and the plasma density is defined by the RF power delivered to the plasma via the capacitive channel. The ‘choice’ of discharge operating mode in experiments is supposedly effected by means of the matching system, because the active and reactive components of the plasma impedance existing in the high and low modes are significantly different. The aforesaid is confirmed by the results of Cunge et al. [49], who demonstrated experimentally the possibility of changing the discharge operating mode by varying the parameters of the matching system.

Figure 14 depicts the power fraction input into the plasma via the inductive channel as a function of the power  $P_{gen}^{ind}$  for different values of  $P_{gen}^{cap}$ . One can see that the power input via the inductive channel depends on the power input through the capacitive channel. For low  $P_{gen}^{ind}$  values, the power  $P^{ind}$  deposited via the inductive channel increases with increasing  $P_{gen}^{cap}$ , then it approaches the values occurring in the absence of the capacitive component, and finally becomes lower than in a purely inductive discharge. The higher the RF power input via the capacitive channel, the stronger is the reduction of the  $P_{pl}^{ind}$  power in the region of high  $P_{gen}^{ind}$  values.

We will qualitatively analyze the mutual influence of the two RF-power input channels by using the equivalent circuit presented in Fig. 15a. Let us consider at first the case of low  $P_{gen}^{ind}$  and low plasma densities. As is known from the literature [38, 49–51] and suggested by simulations, in a wide range of conditions the capacitive discharge phase may exist at a lower power of the RF plasma source than the inductive phase, and some electron concentration  $n_e^*$  is formed in the discharge in this case. It will be recalled that, although the antenna is connected to the ‘inductive’ generator, it is evident that the emergence of plasma in the external circuit of the ‘inductive’

generator gives rise to an equivalent resistance defined in magnitude by  $n_e^*$ , i.e., actually by the RF power delivered via the capacitive channel. When the electron concentration, which is defined by the capacitive channel, exceeds the electron concentration  $n_e^{ind}$  which would exist in the plasma source in the absence of the capacitive channel, the RF-power deposition into the plasma through the inductive channel comes to exceed the input in the absence of the capacitive channel. This is what the solutions presented in Figs 13 and 14 suggest.

Now let us consider the region of high plasma densities. The additional power input via the capacitive channel increases the plasma density; however, in the region of high electron concentrations the equivalent plasma resistance passes through a maximum and begins to decrease (see Section 3). Physically, this is due to impairment of the RF-power penetration into the plasma with increasing plasma density. The position of the maximum of equivalent plasma resistance with reference to electron concentration depends substantially on the magnitude of the magnetic field, and the region of  $P_{gen}^{ind}$  values wherein the power fraction input into the plasma via the inductive channel begins to decrease therefore depends on  $B$  [46].

Naturally, the lowering of the RF-power fraction delivered to the plasma via the inductive channel leads to a decrease in the total power deposited into the plasma (Fig. 14b). In this case, as the power of the RF plasma source feeding the inductive channel increases, the total power approaches the power input via the inductive channel in a purely inductive discharge. It comes as no surprise that the plasma parameters examined experimentally in the high mode

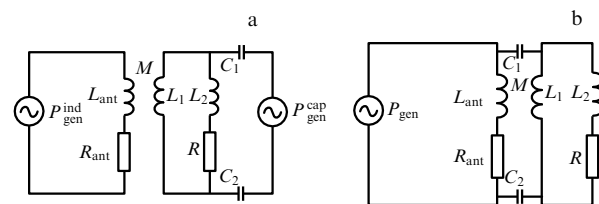


**Figure 15.** Equivalent circuits of an RF discharge maintained by independent inductive and capacitive channels (a) and of a hybrid discharge (b).

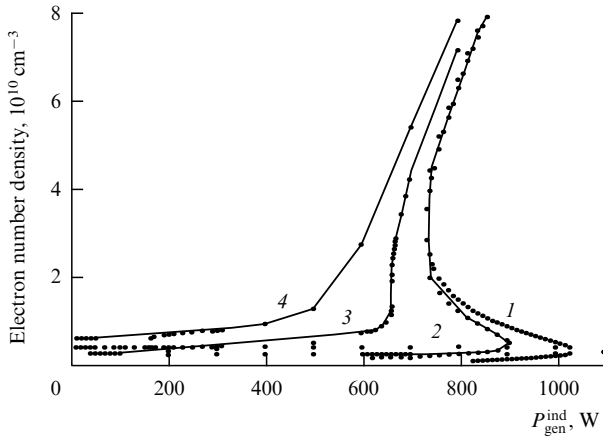


**Figure 16.** Electron concentration as a function of power  $P_{\text{gen}}^{\text{ind}}$  of the RF plasma source feeding the inductive channel for different values of the power  $P_{\text{gen}}^{\text{cap}}$  deposited via the capacitive channel: 1 — 0 W, 2 — 1 W, 3 — 5 W, and 4 — 10 W.

of the purely inductive discharge and the discharge with a capacitive component turned out to be close to each other.

We revert to the region of relatively low  $P_{\text{gen}}^{\text{ind}}$  values, in which a transition from the low discharge operation mode to the high one occurs. As is clear from Fig. 16, in moving from the low plasma density mode to the high density mode at  $P_{\text{gen}}^{\text{cap}} = 0$ , the  $n_e(P_{\text{gen}}^{\text{ind}})$  dependence is characterized by the presence of several solutions, which is commonly attributed to the existence of a hysteresis. However, as  $P_{\text{gen}}^{\text{cap}}$  increases, the inductive-generator power region in which the multivaluedness of solutions exists initially narrows and then vanishes. Furthermore, the threshold power at which the low-to-high mode transition occurs becomes lower. Therefore, mathematical modeling confirmed that the existence of the capacitive channel for the RF-power deposition leads to the disappearance of hysteresis in the  $n_e(P_{\text{gen}}^{\text{ind}})$  dependence. This is related to the increase in the equivalent plasma resistance for low  $n_e$ , when the plasma density is defined by the power input via the capacitive channel.

To summarize the data obtained, it may be inferred that the inductive discharge component is responsible for the emergence of an abrupt transition from the discharge mode with a low electron concentration to the mode with a high concentration. The capacitive discharge component lowers the threshold power whereat this transition occurs and leads to a smoother low-to-high discharge mode transition. The presence of an external magnetic field does not entail qualitative changes to the above conclusions.

## 5.2 Dependence of plasma parameters on the external magnetic field

Let us now consider the effect of the capacitive component on plasma parameters as functions of a magnetic field induction for a fixed RF-generator power. Figure 17 displays the dependences of the argon ion current on the magnetic field induction, which were obtained when a purely inductive discharge, a discharge with independent inductive and capacitive channels, and a hybrid discharge were realized in the ion source. Referring to Fig. 17, in the purely inductive ion source the discharge emerges for a magnetic field induction of about 0.5 mT, the ion current rises with strengthening magnetic field up to 1.3 mT, and then discharge disruption

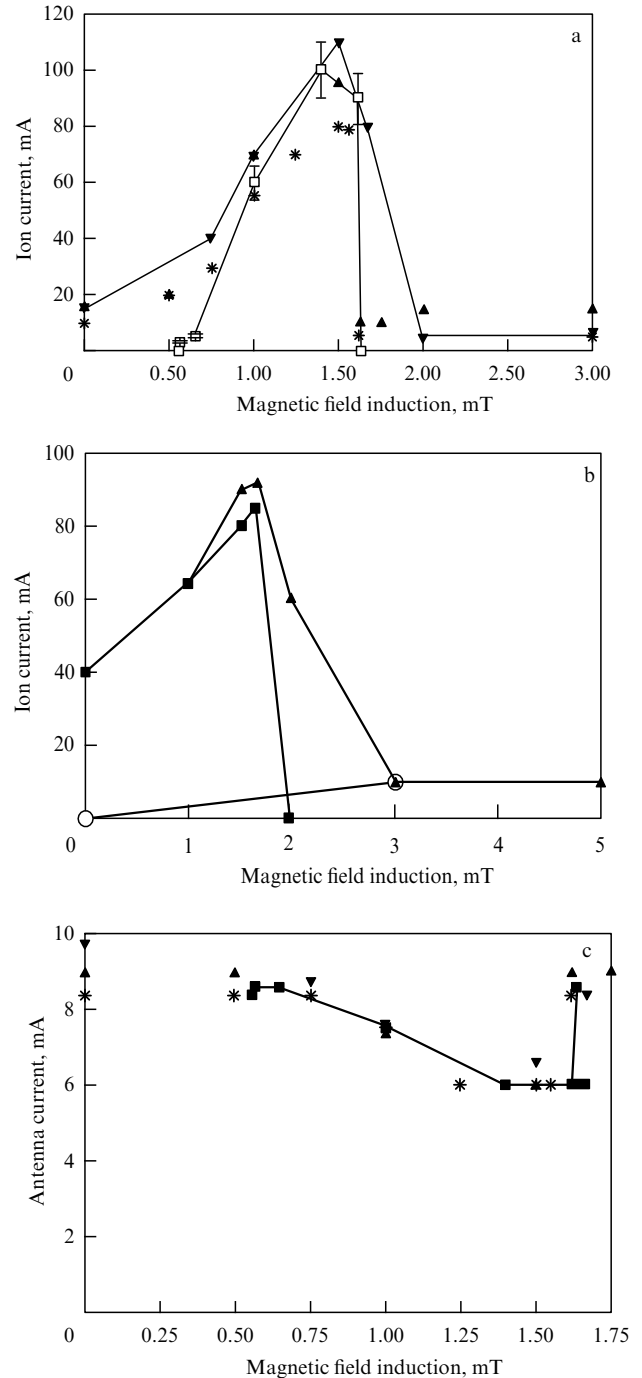


**Figure 17.** Ion beam current (a, b) and antenna current (c) as functions of the magnetic field induction. The squares represent the data for the purely inductive discharge, triangles with vertexes pointing up and down represent the data for the independent capacitive channel fed by an RF-generator power of 60 and 200 W, respectively, the asterisks stand for the hybrid discharge data, and the circles stand for the purely capacitive discharge. The 10-cm long argon ion source had a radius of 5 cm. The flow rate was  $10 \text{ cm}^3 \text{ min}^{-1}$  (Figs 17a and 17c) and  $30 \text{ cm}^3 \text{ min}^{-1}$  (Fig. 17b).

occurs for a magnetic field induction of 1.6 mT. The situation somewhat changes when the power is additionally deposited into the discharge via the independent capacitive channel. The discharge is ignited without any external magnetic field and does not become quenched in the region of disruption of the purely inductive discharge. The discharge passes to the mode characteristic of a purely capacitive discharge, the

transition zone becoming progressively smoother with increasing argon pressure and the RF power deposition into the discharge through the capacitive channel. In the transition regions (for weak magnetic fields and near the discharge disruption), the ion current obtained in the hybrid discharge is close in magnitude to the current obtained in the discharge with an independent capacitive channel and a power of 60 W. In the region of highest ion current (a magnetic field induction of 1.0–1.5 mT), the ion current in the discharge with the independent capacitive channel is somewhat higher than the current typical of the purely inductive discharge, while the ion current in the hybrid discharge is somewhat lower. However, it is pertinent to note that the above difference in current values does not exceed 10–15%.

Figure 17c demonstrates the variation in the antenna current  $I_{\text{ant}}$  upon variation in the magnitude of an external magnetic field for different ways of discharge realization. As would be expected, the difference is greatest in the transition regions; in the region where the ion current peaks, the values of  $I_{\text{ant}}$  obtained in different discharges coincide to within experimental error. This comes as no surprise, because the current carried by the capacitive branch amounted to less than 10% of the antenna current under all the experimental conditions considered.

We now consider the effect of the capacitive component on the dependence of the plasma density on the magnetic field intensity for fixed powers of the RF plasma sources feeding the inductive and capacitive channels. The calculated data are presented in Fig. 18. One can see that the discharge in the presence of the capacitive channel can exist in modes significantly differing in plasma density. In the subsequent discussion we will enlarge on the mode with a high electron concentration. It is clear from Fig. 18 that the discharge becomes quenched for a magnetic field induction of about 8 mT in the absence of the capacitive component. The occurrence of the capacitive component averts discharge disruption and gives rise to the solutions in the magnetic field range where a purely inductive discharge is impossible. Interestingly, the occurrence of a plasma with a density defined by the capacitive component at magnetic fields stronger than 8 mT involves an increase in the power input via the inductive channel, i.e., with  $P^{\text{ind}}$  increasing with  $P_{\text{gen}}^{\text{cap}}$ . The equivalent plasma resistance at low pressures is char-

acterized by an oscillatory dependence on the magnetic field induction. Its oscillatory behavior has the consequence that the fraction of the RF power deposited into the discharge via the inductive channel is nonmonotonically dependent on the magnitude of a magnetic field, which is eventually responsible for the nonmonotonic dependence of the plasma density on the magnetic field intensity. However, for magnetic fields stronger than 8 mT the discharge maintenance and power input via the inductive channel are only possible due to the existence of the capacitive channel of an RF power deposition.

### 5.3 Hybrid discharge

In conclusion, let us qualitatively consider an operation of the hybrid discharge, i.e., the case when the inductive and capacitive channels are connected to the common RF plasma source. A real discharge is modeled in this case, whereat the capacitive channel is formed due to the occurrence of antenna–plasma parasitic capacitances.

Being fully aware of the conventionality of a discharge representation in the form of an equivalent circuit, we nevertheless turn to the consideration of the equivalent discharge circuit depicted in Fig. 15b. The plasma in this circuit is represented in the form of an active load  $R$  and reactive loads  $L_1$  and  $L_2$  incorporated into both the inductive and the capacitive discharge circuits. The RF-generator power goes to heat the antenna, to heat the plasma by induced current, and to heat the plasma in the passage of current through the circuit comprising capacitances  $C_1$ ,  $C_2$  and resistance  $R$  whose magnitude is defined by the ohmic plasma resistance. The magnitudes of capacitances  $C_1$  and  $C_2$  are defined by the surface area of capacitor plates and the plates–plasma distance which is made up of the wall thicknesses and the thickness of the layer between the plasma and the walls of a gas-discharge chamber. For simplicity, it is assumed that a portion of the RF power is completed through the capacitor, while in a real discharge the capacitance between the antenna surface and the plasma operates.

Clearly, the formulation of a self-consistent hybrid-discharge problem in the general case is very complicated. For a hybrid discharge, varying the RF-generator power leads to the self-consistent variation not only in the plasma parameters, but also in the fractions of power deposited into the plasma via the capacitive and inductive channels. However, the interrelationship of these channels may be qualitatively elucidated.

For a low RF-generator power, when a purely inductive discharge cannot occur, a discharge ignites in the capacitive mode. Power equal to the RF-generator power is deposited into the plasma via the capacitive channel, with the exception of losses for antenna heating. This gives rise to a nonzero equivalent resistance in the inductive circuit and to a power deposition into the plasma through the inductive channel. We emphasize that the magnitude of the power contribution via the inductive channel is determined by the power delivered to the plasma via the capacitive channel. The plasma density depends on the total power delivered to the plasma via both channels. Clearly, in this case it is physically illegitimate to treat the occurring low-density discharge mode as purely capacitive, because the total power deposition into the plasma is governed not only by the capacitive channel, but by the inductive channel, as well.

At higher generator powers, when the electron concentration is defined by the power fraction delivered via the

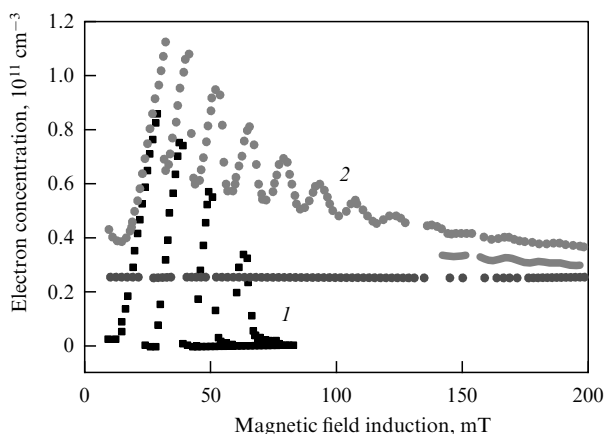


**Figure 18.** Electron concentration as a function of the magnetic field induction for a fixed RF-generator power  $P_{\text{gen}}^{\text{ind}}$  (200 W) feeding the inductive channel at a power  $P_{\text{gen}}^{\text{cap}}$  input via the capacitive channel: 1 — 0, and 2 — 50 W.

inductive channel, the behavior of a hybrid discharge is qualitatively close to the behavior of a discharge with independent channels of RF-power input. In the region of high electron concentrations, where the equivalent plasma resistance begins to lower with increasing  $n_e$ , the part played by the capacitive component becomes significant. Therefore, it may be inferred that the mode of the inductive discharge with a high electron concentration is not purely inductive. The capacitive component has a pronounced effect on the magnitude of the power delivered to the plasma via the inductive channel.

Therefore, the occurrence of the capacitive discharge component changes the fraction of power deposited into the plasma via the inductive channel. This shifts the position of the low-to-high discharge mode transition to the domain of lower RF-generator powers. In going from the low to the high discharge mode, the presence of the capacitive component reveals itself in a smoother plasma density variation with increasing generator power and in the disappearance of hysteresis. Due to the power input through the capacitive channel, the electron concentration exceeds the magnitude whereat the equivalent resistance reaches its peak, with the consequential decrease in the RF-power input via the inductive channel. That is why it is physically illegitimate to compare the low- and high-electron-concentration modes of the RF inductive discharge with the capacitive and inductive modes, since the existence of one power-input channel results in a change of the fraction of power delivered to the plasma through the other channel.

## 6. On the feasibility of optimizing low-pressure inductive plasma sources

By taking advantage of the results outlined in Sections 2–5, we will endeavor to provide answers to the questions concerning the development of new RF plasma sources, which were posed in the Introduction. First of all we shall analyze the feasibility of optimizing the RF-power deposition into the plasma. It will be assumed that the RF-generator power is totally transferred by means of a matching system to the external circuit which consists of an antenna and the plasma. As shown in Section 4, the RF-generator power in real experiments is distributed between two channels: the plasma, and the elements of the external circuit, which possess active resistances, with the power fraction absorbed by the plasma depending on the parameters of the plasma source itself. This may be the cause of the low efficiency, as well as the irreproducibility, of the operation of plasma sources when used in facilities with different matching systems, assembling flanges, etc. To ensure highly efficient and reproducible operating regimes of the plasma sources, it is requisite that

$$P_{\text{gen}} \approx P_{\text{pl}} \gg P_{\text{ant}}, \quad (20)$$

which is equivalent to the requirement

$$R_{\text{pl}} \gg R_{\text{ant}}. \quad (21)$$

The simplest solution to the problem is to lower the effective antenna resistance. However, it is not always possible to substantially decrease  $R_{\text{ant}}$ . The data of experimental investigations [33, 52, 53] into the efficiency of RF-power deposition into the plasma show that the effective resistance  $R_{\text{ant}}$  of the external circuit, measured in differently

staged experiments, ranges between 0.2 and 3  $\Omega$ . In this case, the low  $R_{\text{ant}}$  values are characteristic of experiments performed with gas-discharge glass tubes sufficiently remote from the metal elements of the facilities.

We now consider the absolute values of the equivalent plasma resistance and begin with a discharge without a magnetic field. Calculations showed [54] that the absolute values of the equivalent resistance increase progressively with the source radius; however, even the maximum value of the equivalent plasma resistance for a source of radius 50 cm is only little higher than 1  $\Omega$ . This signifies that at most 30% of the power imparted by the RF plasma source to the external circuit can be deposited into the low-pressure plasma produced by a source of radius 2.5 cm for an external circuit resistance of 1  $\Omega$ ; in this case, the residual 70% of the power will go to heat the antenna, the elements of the matching system, etc. Increasing the source radius improves the result; however, in this case, too, it is hardly possible to attain a deposition of at least 80% of the RF-generator power into the plasma.

With the purpose of finding new vistas to increase the equivalent plasma resistance under inductive excitation of a discharge without a magnetic field, calculations of  $R_{\text{pl}}$  with increasing argon pressure were carried out at different frequencies [54]. The data showed that increasing pressure leads to a significant rise in the equivalent resistance. The optimal operating frequency of RF plasma sources depends on the electron concentration required to accomplish a technological task. When it is required to develop a device operating at plasma densities  $10^{10} \leq n_e \leq 10^{11} \text{ cm}^{-3}$ , the optimal RF-power deposition into the plasma may be effected with operating frequencies of 6–13 MHz. When higher plasma densities are required, viz.  $10^{11} \leq n_e \leq 10^{12} \text{ cm}^{-3}$  and  $n_e > 10^{12} \text{ cm}^{-3}$ , typical of plasma reactors employed for semiconductor etching, it is expedient to raise the frequency to 27 MHz and 40 MHz, respectively.

We now consider the data obtained for a discharge with an external magnetic field. For low pressures, the equivalent plasma resistance in this case is substantially higher than that obtained in the absence of a magnetic field. As in the case of RF inductive plasma sources without a magnetic field, the equivalent resistance rises with increasing plasma source radius and for  $R \geq 10$  cm supplies a nearly complete absorption of the RF power imparted by the generator to the external circuit. While the equivalent resistance is independent of the plasma source length for disk-shaped plasma sources in the absence of an external magnetic field,  $R_{\text{pl}}$  may rise with increasing gas-discharge chamber length for an elongated cylindrical source. Calculations revealed that this may prove to be helpful in the development of short-radius devices for which the values of  $R_{\text{pl}}$  are small, as well as for RF sources without a magnetic field.

Another parameter which permits increasing  $R_{\text{pl}}$  is the operating frequency  $\omega$  of an RF plasma source. Calculations showed that rising  $\omega$  leads to a substantial increase in  $R_{\text{pl}}$ ; in this case, however, the peak of the  $R_{\text{pl}}(B)$  function shifts towards stronger magnetic fields. Furthermore, pronounced oscillations of the resistance are observed as the magnetic field is strengthened.

Earlier it was noted that raising the working gas pressure leads to an increase in equivalent plasma resistance of an RF inductive discharge without a magnetic field. As noted in Section 3, the situation is precisely the opposite for the magnetic fields corresponding to the helicon and TG wave

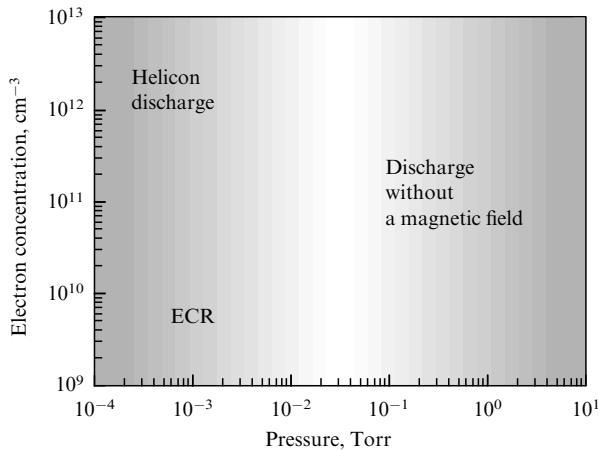


**Figure 19.** Plasma parameter domains wherein it is possible to deposit into the plasma the largest RF-power fraction for different ways of inductive discharge excitation in the operation at a frequency of 13 MHz.

excitation domain — the peak values of  $R_{pl}$  decrease with an increase in the magnetic field induction. This fact argues for the inclusion of ‘helicon’ RF-discharge regimes in the development of low-pressure plasma sources.

The values of equivalent resistance obtained for different ways and conditions of plasma excitation permit formulating several conclusions about the possible vistas for improving the efficiency of RF power deposition into low-pressure plasmas. Figure 19 exhibits the domains of plasma parameters whereat it is possible to deposit into the plasma the largest RF-power fraction for different ways of inductive discharge excitation in the operation at a frequency of 13.6 MHz. As noted above, the best way of organizing the discharge at gas pressures higher than  $10^{-2}$  Torr points to the inductive discharge without a magnetic field, which is dominated by the collisional mechanism of RF-power absorption. Lowering the pressure and thereby diminishing the part played by collisional mechanisms of RF-power absorption generate the need for enhancing the collisionless absorption of RF power, which is possible under ECR in the region of low electron concentrations, and in the excitation of helicons and TG waves in the higher-concentration region. In the low-pressure range, the RF power is better deposited into sources with a long radius; the efficiency of RF-power deposition into short-radius sources may be improved by increasing either the source length or the operating frequency.

Plasma sources intended for higher electron concentrations should be equipped with a magnetic system producing stronger magnetic fields than the sources meant for lower plasma densities.

Clearly, the discharge disruptions and the hysteresis in the plasma parameters as functions of the external factors that influence discharge operation are highly undesirable effects from the standpoint of the organization of the operating regimes of inductive plasma sources. When the effective antenna resistance is high, it is expedient to employ the capacitive discharge component, which permits stabilizing the plasma.

The possible solutions to the problem of producing the highest possible plasma density for a given deposited power are well known from the physics and engineering of plasma and ion sources fed by dc voltage sources [55]. For a given power level, the plasma density may be increased by selecting

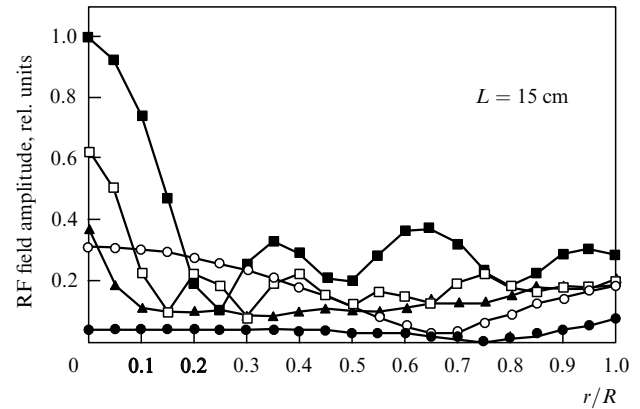


**Figure 20.** Calculated radial distribution of the RF field amplitude upon changes in the induction of an external magnetic field for 15-cm long plasma sources with a radius  $R = 7.5$  cm: ● —  $B = 1$  mT, ○ —  $B = 2.5$  mT, ■ —  $B = 3.5$  mT, □ —  $B = 5$  mT, and ▼ —  $B = 10$  mT.

the optimal length–diameter ratio for the plasma source, as well as the configuration and magnitude of the external magnetic field. However, these conditions should be matched to the conditions for efficient RF-power absorption in the case of RF plasma sources. As a rule, this leads to significant changes in the optimal structural parameters of the plasma sources [54].

As noted in Section 4, varying the intensity of an external magnetic field leads to a spatial redistribution of the plasma density. Figure 20 depicts the calculated radial dependences of the RF electric fields, obtained for different values of the magnetic field induction [46]. One can see that the electric wave fields penetrate into the plasma interior for magnetic fields close in magnitude to the value  $B_{max}$ , which corresponds to the peak of electron concentration, while the waves transform to surface waves for magnetic field intensities substantially lower and higher than  $B_{max}$ . This property is inherent in relatively lengthy plasma sources [46]. In short plasma sources, only surface waves are present for any magnitudes of the magnetic field [46]. The Larmor radius estimated for sub-10 eV electrons, which constitute the majority of plasma electrons, in magnetic fields stronger than 1 mT does not exceed 1 cm. This gives grounds to believe that the RF-power deposition into the plasma is locally effected in the radial direction. Therefore, the spatial plasma density distribution may be varied by changing the magnitude of the external magnetic field and the length of the gas-discharge chamber. The most uniform plasma may be obtained by employing a magnetic field close in magnitude to  $B_{max}$  whereat the equivalent plasma resistance reaches its peak.

## 7. Conclusion

Both experimental and theoretical data obtained in recent years suggest that the parameters of RF inductive discharge plasmas depend on the power loss in the external circuit and the amounts of power delivered into the discharge via the inductive and capacitive channels. On the one hand, the plasma parameters are defined by the amounts of absorbed power, and, on the other hand, determine themselves both the ratio between the amounts of power delivered via different channels and eventually the power absorbed by the plasma.

This underlies the self-consistent discharge nature. The self-consistency manifests itself most obviously in discharge disruptions and the strong nonmonotonicity of the dependence of plasma parameters on the magnetic field intensity. Substantial power losses in the external circuit and the nonmonotonic density dependence of the plasma capacity to absorb the RF power are responsible for the saturation of the plasma density with increasing RF-generator power and the emergence of a hysteresis in the dependence of plasma parameters on the RF-generator power and the magnitude of an external magnetic field.

The occurrence of a capacitive discharge component gives rise to a variation in the fraction of power deposited into the plasma via the inductive channel. This displaces the position of the low-to-high discharge mode transition towards a lower RF-generator power range. In moving from the low discharge mode to the high one, the occurrence of the capacitive component shows up in a smoother variation of the plasma density with increasing the generator power and in the disappearance of the hysteresis. The increase, due to the power input via the capacitive channel, in the electron concentration to values exceeding the concentration whereat the equivalent plasma resistance reaches its peak has the effect that the RF-power deposition via the inductive channel decreases. It is physically illegitimate to compare the low- and high-electron-concentration modes of the RF inductive discharge with the capacitive and inductive modes, because the existence of one power-input channel results in a change of the power fraction delivered to the plasma via the other channel.

Refinement of the picture of physical processes in a low-pressure RF inductive discharge permits optimizing the parameters of the plasma devices operating on its basis.

**Acknowledgments.** The author is deeply grateful to Anri Amvrosievich Rukhadze and Andrei Fedorovich Aleksandrov for their constant interest, numerous discussions, and helpful remarks made in the reading of the manuscript.

## References

- Thomson J J *Philos. Mag.* **32** 321 (1891)
- Hittorf W *Ann. Phys. Chem.* **21** 90 (1884)
- Townsend J S, Donaldson R H *Philos. Mag.* **5** 178 (1928)
- Townsend J S, Donaldson R H *Philos. Mag.* **7** 600 (1929)
- MacKinnon K A *Philos. Mag.* **8** 605 (1929)
- Godyak V A "Plasma phenomena in inductive discharges", in *Invited Papers from the 30th European Physical Soc. Conf. on Controlled Fusion and Plasma Physics (St.-Petersburg, Russia, 7–11 July 2003)*; *Plasma Phys. Control. Fusion* **45** A399 (2003)
- Hopwood J *Plasma Sources Sci. Technol.* **1** 109 (1992)
- Loeb H W "Recent work on radio frequency ion thrusters" *J. Spacecraft Rockets* **8** 494 (1971)
- Godyak V A, Alexandrovich B M, Piejak R B, US Patent No. 5,834,905 (November 19, 1998)
- Stevens J E "Electron cyclotron resonance plasma sources", in *High Density Plasma Sources: Design, Physics, and Phenomena* (Ed. O A Popov) (Park Ridge, NJ: Noyes Publ., 1995) p. 312
- Uchida T *Jpn. J. Appl. Phys.* **33** L43 (1994)
- Tsuboi H et al. *Jpn. J. Appl. Phys.* **34** 2476 (1995)
- Yoshida Z, Uchida T *Jpn. J. Appl. Phys.* **34** 4213 (1995)
- Uchida T *J. Vac. Sci. Technol. A* **16** 1529 (1998)
- Uchida T, Jpn. Patents Nos 07-090632, 08-078188, 07-263190 (1994)
- Arsenin A V, Leiman V G, Tarakanov V P *Kratk. Soobshch. Fiz.* (4) 19 (2003) [*Bull. Lebedev Phys. Inst.* (4) 15 (2003)]
- Boswell R W, US Patent No. 4,810,935 (March 7, 1989)
- Chen F F "Helicon plasma sources", in *High Density Plasma Sources: Design, Physics, and Phenomena* (Ed. O A Popov) (Park Ridge, NJ: Noyes Publ., 1995) p. 1
- Aleksandrov A F et al. *Prikl. Fiz.* (1) 3 (1995)
- Aleksandrov A F et al., RF Patent No. 2095877
- Silin V P, Rukhadze A A *Elektromagnitnye Svoistva Plazmy i Plazmopodobnykh Sred* (Electromagnetic Properties of Plasmas and Plasma-Like Media) (Moscow: Gosatomizdat, 1961)]
- Ginzburg V L, Rukhadze A A *Volny v Magnitoaktivnoi Plazme* (Waves in Magnetoactive Plasma) (Moscow: Nauka, 1970)
- Aleksandrov A F, Bogdankevich L S, Rukhadze A A *Osnovy Elektrodinamiki Plazmy* (Principles of Plasma Electrodynamics) (Moscow: Vysshaya Shkola, 1978) [Translated into English (Berlin: Springer-Verlag, 1984)]
- Kondratenko A N *Proniknovenie Polya v Plazmu* (Field Penetration into a Plasma) (Moscow: Atomizdat, 1979)
- Lieberman M A, Lichtenberg A J *Principles of Plasma Discharges and Materials Processing* (New York: Wiley, 1994)
- Boswell R W *Phys. Lett. A* **33** 457 (1970)
- Boswell R W *Plasma Phys. Control. Fusion* **26** 1147 (1984)
- Boswell R W, Henry D *Appl. Phys. Lett.* **47** 1095 (1985)
- Chen F F *Plasma Phys. Contr. Fusion* **33** (4) 339 (1991)
- Kolobov V I, Economou D J *Plasma Sources Sci. Technol.* **6** R1 (1997)
- Chen F F *Phys. Plasmas* **8** 3008 (2001)
- Godyak V A, Piejak R B, Alexandrovich B M *Plasma Sources Sci. Technol.* **11** 525 (2002)
- Miljak D G, Chen F F *Plasma Sources Sci. Technol.* **7** 61 (1998)
- Blackwell D D, Chen F F *Plasma Sources Sci.* **10** 226 (2001)
- Chen F F *Plasma Phys. Control. Fusion* **33** 339 (1991)
- Aleksandrov A F et al. *Zh. Tekh. Fiz.* **64** (11) 53 (1994) [*Tech. Phys.* **39** 1118 (1994)]
- Shamrai K P, Taranov V B *Plasma Sources Sci. Technol.* **5** 474 (1996)
- Turner M M, Lieberman M A *Plasma Sources Sci. Technol.* **8** 313 (1999)
- Thomson J J *Philos. Mag.* **4** 1128 (1927)
- Piejak R B, Godyak V A, Alexandrovich B M *Plasma Sources Sci. Technol.* **1** 179 (1992)
- Aleksandrov A F et al. *Fiz. Plazmy* **30** 434 (2004) [*Plasma Phys. Rep.* **30** 398 (2004)]
- Vavilin K V et al. *Zh. Tekh. Fiz.* **74** (5) 44 (2004) [*Tech. Phys.* **49** 565 (2004)]
- Vavilin K V et al. *Zh. Tekh. Fiz.* **74** (6) 25 (2004) [*Tech. Phys.* **49** 686 (2004)]
- Vavilin K V et al. *Zh. Tekh. Fiz.* **74** (6) 29 (2004) [*Tech. Phys.* **49** 691 (2004)]
- Vavilin K V et al. *Fiz. Plazmy* **30** 739 (2004) [*Plasma Phys. Rep.* **30** 687 (2004)]
- Aleksandrov A F et al. *Prikl. Fiz.* (4) 70; (5) 72 (2005); (1) 36; (2) 41; (4) 54; (5) 33; (5) 39 (2006)
- Godyak V A, Piejak R B, Alexandrovich B M *J. Appl. Phys.* **85** 703 (1999)
- Godyak V A, Piejak R B, Alexandrovich B M *Plasma Sources Sci. Technol.* **3** 169 (1994)
- Cunge G et al. *Plasma Sources Sci. Technol.* **8** 576 (1999)
- El-Fayoumi I M, Jones I R, Turner M M *J. Phys. D: Appl. Phys.* **31** 3082 (1998)
- Suzuki K et al. *Plasma Sources Sci. Technol.* **7** 13 (1998)
- Godyak V *Plasma Phys. Control. Fusion* **45** A399 (2003)
- Lee H-J, Yang I-D, Whang K-W *Plasma Sources Sci. Technol.* **5** 383 (1996)
- Aleksandrov A F et al. "On the possibilities of RF ion thrusters optimization", in *Proc. of the 29th Intern. Electric. Propulsion Conf. (IEPCO5), Princeton, NJ, October 31 – November 4, 2005*
- Kozlov N P, Morozov A I (Eds) *Plazmennyye Uskoriteli i Ionnyye Inzhektory* (Plasma Accelerators and Ion Injectors) (Moscow: Nauka, 1984)